LQG - BASED FUZZY LOGIC CONTROL OF ACTIVE SUSPENSION SYSTEMS

Thesis

Submitted to

Graduate Engineering & Research

School of Engineering

UNIVERSITY OF DAYTON

In Partial Fulfillment of the Requirements for

The Degree

Master of Science in Mechanical Engineering

By

Mahesh N. Ariyakula

UNIVERSITY OF DAYTON, Ohio

August, 1996

LQG - BASED FUZZY LOGIC CONTROL OF ACTIVE SUSPENSION SYSTEMS

APPROVED BY:

A.R. Kashani, Ph.D.
Associate Professor
Mechanical & Aerospace Engr. Dept.
Advisory Committee, Chairman

George Doyle, Ph.D.
Associate Professor
Mechanical & Aerospace Engr. Dept.
Committee Member

Malcolm W. Daniels, Ph.D.
Assistant Professor
Electrical Engr. Dept.
Committee Member

Donald L. Moon, Ph.D.
Associate Dean
Graduate Engineering Program & Research
School of Engineering

Joseph Lestingi, D. Eng., P.E.
Dean
School of Engineering

ACKNOWLEDGEMENTS

Foremost, I am indebted to Dr. A.R. Kashani for his technical support and guidance he provided as my advisor during this research, for which I shall relish in the years to come. I also appreciate the revisions (papers) of Peter S. Meybeck and Mikell K. Eiler.

A special thanks to Dr. John McCloskey who guided me well in finishing a part of my thesis.

I dedicate this thesis to my family members, friends and well wishers, whom I thank for their love and encouragement.

Mahesh Ariyakula

ABSTRACT

LQG - Based Fuzzy Logic Control of Active Suspension Systems

Name: **Mahesh N. Ariyakula,**

University of Dayton, 1996

Advisor: **Dr. A.R. Kashani**

The importance in the introduction of an active element in an automotive suspension is to negate the problem of trade-off between comfort and handling. This work proceeds with a comprehensive review of publications on this particular objective in the design of active suspension systems, providing an insight of the research in the last 27 years.

An indepth discussion of the latest and most advanced techniques as of today to improve comfort and handling (enhancing mobility) simultaneously, i.e. LQR and LQG optimal control techniques are shown. However contemplating them to be inappropriate in the design of active suspension systems, focus is targetted on improvising upon the proposed control strategy.

A new technique based on Fuzzy Logic thinking is explored. The control technique deals with discrete Kalman estimators which are difficult to implement in large numbers, like in a full car, which adds to the real time computational load. Even if done so, all the controllers do not contribute to the final control output simultaneously, hence a thorough study is conducted on Kalman estimators leading to LQG based control and suggestions are made to have a moving bank to rectify this problem in future. The main terms contributing to the nonlinearities of the suspension model are kinematic constraints

on motion, as well as, damping and stiffness of the tires. Considering coefficients of damping and stiffness of the tires as uncertain parameters which can assume a set of possible values, a collection of linear models are developed that can, collectively, describe the suspension. This leads to conception and implementation of a multiple bank of estimators and controllers to take care of model variation.

The implementation of the controller on the original nonlinear model (in ADAMS), for tuning, and subsequently on the test rig is currently underway.

TABLE OF CONTENTS

LIST OF FIGURES

LIST OF TABLES

CHAPTER I

INTRODUCTION

The main objective of active suspension for off-road vehicles is reducing the power absorbed by the occupants. Absorbed power is related to the time integral of squared acceleration (weighted in frequency by human response transfer function) [22]. This makes linear quadratic regulators appropriate for active suspension control of these vehicles, with the filtered sprung mass acceleration being the main component of the objective (cost) function. To assure that this objective i.e., lowering the acceleration, is not compromising the vehicle stability, suspension working space, and control energy, these terms are also added to the objective function.

Active car suspension is an expanding field in the design of cars in the luxury class. It is already available on cars like Nissan's Infinity Q45, Toyota's Celica GT-R AS, or Chevrolet's Corvette ZR1 [36]. Nissan compares its Infinity Q45 to a cheetah, running over rough terrain while its body remains parallel to the horizon. The brain of the hardware of active car suspension is a microprocessor implementing the control algorithm (see Figure 1.1). The controller drives pressure control valves between actuator and power source. The actuator is located between wheel base and body, allowing to apply a force between both elements and capable of changing the states of the car. Both states and external disturbance changes are monitored by sensors which provide the

necessary information for the controller.

Design of controllers for active suspensions using optimal control theory (linear quadratic techniques, in general, and linear quadratic Gaussian, LQG, in particular) has enjoyed a broad acceptance amongst the active suspension research community, see for example ([10], [12], [16] and [30]). LQG is a computationally elegant, time domain, linear quadratic control technique using state estimates which are provided by a Kalman filter. The use of model-based estimated states causes the performance and stability characteristics of LQG controlled systems deteriorate, sometimes drastically, when the linear model deviates from the plant. This is mainly due to the use of excessive estimator gain to compensate for the modelling errors.

The above mentioned lack of stability robustness associated with LQG control can be addressed by adding loop transfer recovery (LTR) to the LQG controller ([30] and [16]) or using a more robust control technique such as H-∞ [17]. These solutions achieve better stability characteristics at the expense of system performance. Moreover, lowering the absorbed power (which is a time integral concept) is more in line with LQ controllers than with H-∞ ones. The other alternative is staying with LQG but using multiple models, rather than one, describing the plant. Using the former approach a bank of estimators (Kalman filters) and controllers are designed based on these models. The combination of these estimators and their corresponding controllers can be viewed as a collection of LQG controllers in parallel. In this scheme, weighted average of all the controllers will be the control input to the plant. The use of a bank of Kalman filters in this control strategy will alleviate the need for opening the bandwidth of the estimation which is the main reason for low stability robustness characteristics of LQG control. [23]

has used conditional probability concepts for evaluating the weighting factors. Since probability describes the uncertainity of event occurance, not the degree to which the event occurs (which is described by fuzziness), we take fuzzy logic approach to evaluate the weights for averaging the output of each controller in the bank.

The potential problem with multiple model control technique is the large number of LQG controllers in the bank. Although this is not a concern in control of the quarter car suspension, but it will be in control of the full car suspension. The fact is that at any instant in time, only a few of the controllers in the bank contribute to the control output, in a meaningful way. In the extension of this work to quarter car suspension control itself, another fuzzy decision making logic is used in choosing the subset of contributing controllers and moving the subset inside the set of all controllers.

Need and Motivation for Active Car Suspension

Performance criteria of a car suspension contain a broad spectrum of objectives; a review and summary of objectives can be found in [28]. The performance criteria include working space (also found as rattlespace, see [12]), road contact (also called wheel load variation [28]), grip and discomfort. Discomfort is defined as sprung mass acceleration [22], as weighted sprung mass acceleration [28], or as jerk of the sprung mass [11]. Throughout this work sprung mass acceleration will be used as a measurement for discomfort. Additional criteria are static and dynamic attitude behaviour, roll and pitch behaviour, contribution to good steering behaviour, actuator force levels, and power consumption. Among practitioners, however, stability and failure safety are the most important aspects. As long as the active system is not guaranteed to be failure safe and robust, there is no practical sense in improving other performance criteria.

It is well known, that in common suspension design there is a trade-off necessary. Decreasing passenger discomfort, i.e. a soft ride, will increase the wheel load variation, decreasing the road contact, whereas increasing the road contact i.e. a sporty ride will increase passenger discomfort. There is no possibility in improving both of them. This problem triggered off for an alternate strategy in the late sixties to examine the influence of placing an active element in parallel with the passive suspension part. This new technique of active suspension system opens the chance of changing the system properties in a way which cant be achieved by changing the parameters of the passive suspension. This becomes more obvious when one considers the following example. Let the car be described by the so called quarter car model in Figure 1.2. The details of the model are given. This 2-degree-of-freedom (2-DOF) system is of 4th order. With pole placement it is possible to place all four eigen values anywhere in the s-plane. This is not possible with just the passive element. If done so, unrealistic values of mass of car body M, mass of wheel base m, suspension stiffness K and suspension damping coefficient C are obtained.

Inclusion of an active element and a suitable control law, e.g. pole placement, the desired pole locations can be obtained without unrealistic values for M, m, K or C. There is no proof that active suspension will overcome the dilemma between comfort and road contact, but it shows that active suspension opens the door for a variety of new possibilities.

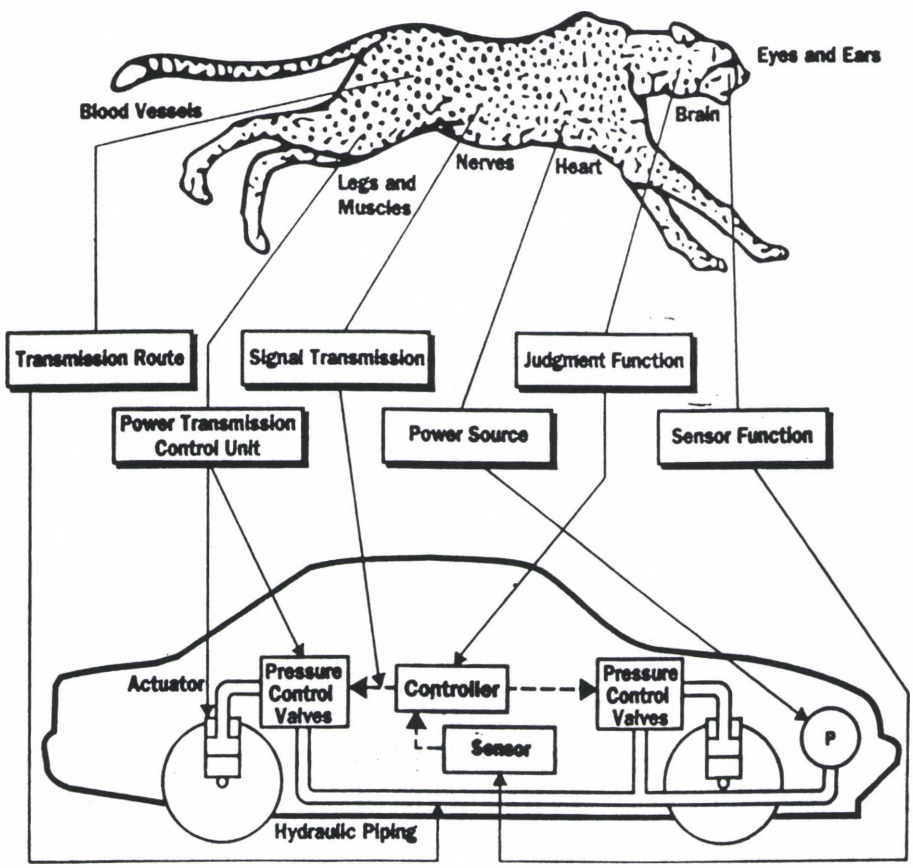

Figure 1.1 - Concept Of Active Car Suspension

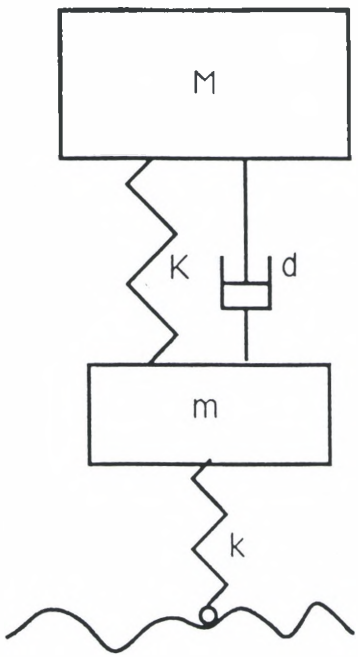

Figure 1.2 (a) - Quarter Car Representation Of A Passive Suspension

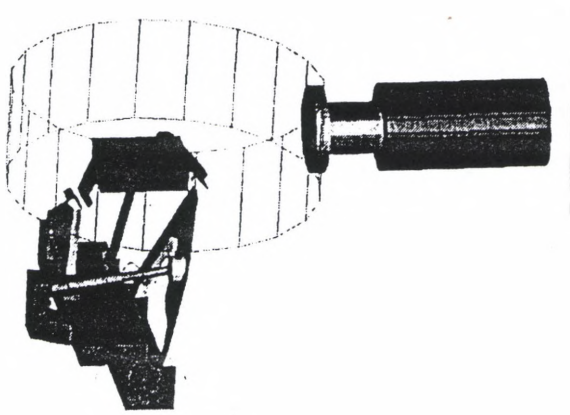

(b) Adams Model Of The Suspension

Quarter Car Suspension Modelling

Detailed Modelling

The simplest and commonly used model, which allows discomfort and road contact in the automotive suspension design is the quarter car or corner car representation shown in Figure 1.2. A quarter car test rig simulating the vehicle's rear right station is constructed. To test different control algorithms, prior to implementation on the test rig the model of the quarter car is developed in ADAMS; see Figure 1.2 (a). This representation is perfect for low frequencies unlike high frequencies which bias the approximations of the corner car model due to coupling of the wheel stations and flexible modes, are small in amplitude and therefore not as important.

The sprung mass is constrained to move only in the vertical direction, as it is on the test rig. The test rig is constructed with friction reducing surfaces along the two square guide posts to provide this constraint. There will be a slight friction associated with this movement that is not modelled. In the assembly of the test rig, care is taken to ensure that the center of mass is located in the plane of these guide posts to minimize moment loading of the constraint; the center of mass of the sprung mass was similarly placed in ADAMS model.

The corner car suspension model is so chosen in this work because the studied objectives are comfort and road contact and also due to the ease of design and computation. As the quarter car model contains only a few parameters and has only one input, design, computation and understanding of the relation between design and results are easier compared to that of a full car model.

The quarter car suspension model consists of two masses, one representing the car body mass M and the other representing the mass of axle and wheel, m, a suspension unit and a spring representing the tire. The suspension unit comprises of a coil spring with stiffness K and a dash-pot with damping coefficient C and an ideal actuator, i.e. an actuator with a bandwidth higher than the frequency range of interest. Considering the dynamics of the hydraulic actuator would add to the complexity of design and computation, but it does not alter the performance criteria nor the model. Throughout the literature on active suspension, being referenced in this work, actuator dynamics are neglected.

The tire is modelled as a single component force using an ADAMS impact function. Only Z-axis dynamics are considered as the test rig has a slide table mounted on the top of the road profile actuator. This slide table will minimize side loading of the road-simulating actuator and eliminates the need to model lateral tire forces at this stage. similar to that of a suspension unit, with tire stiffness K_t, and damping coefficient, C_t. The justification of tire modelling as a spring and dashpot is found in [28].

The tire force has two components, a stiffness component and a viscous damping one. The stiffness force, f_k, is a function of the tire deflection, x_2, defined as the relative position of the tire with respect to the road, measured from its unloaded position. As the tire deflects there is a non-linear stiffening effect due to the nature of the rubber and the geometry of the tire. To accurately model this phenomenon a deformation force exponent, e, is used. The stiffness component of the tire force is then evaluated according to Equation 1.1

$$f_k(x_2) = k' x_2^e \quad (1.1)$$

where x_2 is the tire deflection in mm and fk is the tire stiffness force in N. Based on experimental data the coefficient, k', was chosen to be 85, and the deformation force exponent, e, was chosen to be 1.3.

The damping coefficient of the tire force is modelled as a cubic polynomial function of the tire deflection to prevent discontinuity at the initial contact between the tire and the road profile actuator. Thus, the damping coefficient is zero, at zero deflection and maximum, C_{max} , at a user defined deflection. Based on data from (Wong, 1978), for this type of a tire the maximum vertical damping coefficient, C_{max}, is approximately 0.73 Ns/mm. The deflection at which damping reaches a maximum was more arbitrarily chosen to be 38 mm. The cubic polynomial describing the damping coefficient of the tire is shown in Equation 2

$$C_t(x_2) = 1.5 * 10^{-3} x_2^2 - 2.66 * 10^{-5} x_2^3 \quad (1.2)$$

where the tire deflection x_2 is in mm and tire damping coefficient c_t is in Ns/mm. Stiffness force and damping coefficient of the tire are shown in Figure 1.2(b). For tire deflections higher than 38 mm, ct is considered constant at its value evaluated at x_2 = 38 mm.

The suspension actuator is modelled as a single component force. The dynamics of hydraulic actuation is interfaced with ADAMS in a user-defined code.

Control Modeling

Lagrange multiplier can be used to formulate the nonlinear equations of motion constrained by the double-A arm mechanism. When heave is the motion of interest, which is true in quarter car rigs, the constraints on motion can be accounted for by

modifying the stiffness and damping coefficient of the suspension spring and dashpot. In light of this, spring and dashpot forces were analyzed independently, in the ADAMS model as described in the following.

The damping of the shock absorber was set to zero and the frame was fixed to the ground. Then the wheel was displaced through the entire rattlespace. The sum of the forces acting in the vertical direction on the sprung mass at the spring mount and the joint connecting the upper and lower control arms were plotted vs. the wheel travel, and observed to be very linear. The slope of that line is taken as the unconstrained spring rate of K= 27.4 N/mm. Note that the original stiffness of the spring used in the non linear ADAMS model was 167 N/mm. Next, the shock absorber damping coefficient was restored back to 10 Ns/mm and the spring stiffness was set to zero. Having gone through the similar analysis as presented above, the sum of the forces acting on the sprung mass vs. unsprung mass velocity (wheel travel velocity) was derived in ADAMS and observed to be linear, as well. The slope of this line, C = 1.65 Ns/mm, is taken as the unconstrained damping coefficient. Again, it should be emphasized that this damping coefficient is different from the original damping coefficient of 10 Ns/mm used in the ADAMS model. Using the equivalent values of suspension spring stiffness and shock absorber damping coefficient, i.e., K and C, we can approximate the constrained motion of the corner car ADAMS model with the model shown in Figure 1.2(c). The state variable formulation of the model is described below.

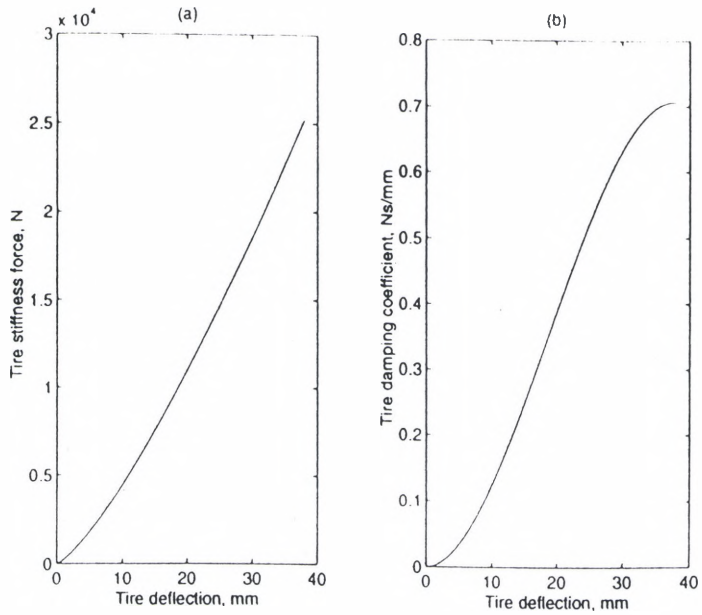

(c) Tire Stiffness And Damping Coefficient As A Function Of Tire Deflection

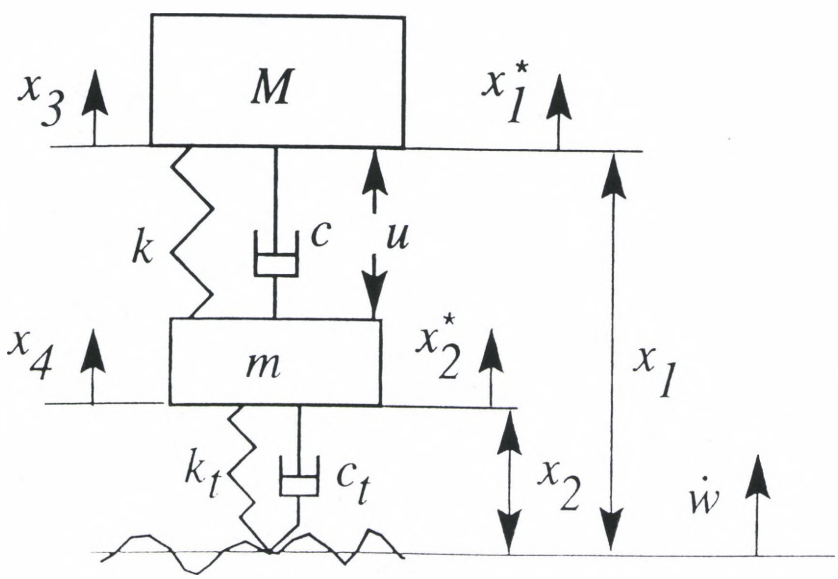

(d) Quarter Car Model

The positions of sprung and unsprung masses where the suspension and tire springs are not loaded are considered as the references for displacement measurements. As shown in Figure 1.2(c), the reason for this choice of position references is that the tire stiffness and damping characteristics are given as functions of unloaded tire deflection. Considering the absolute positions of the sprung and the unsprung masses as x_1^* and x_2^*, the states are selected as x_1 being the relative position of the road surface and the sprung mass ($x_1 = w - x_1^*$), x_2 being the relative position of the road surface and the unsprung mass ($x_2 = w - x_2^*$), x_3 and x_4 being the absolute velocities of the sprung and unsprung masses, respectively, and w is the road profile. State variable formulation of the system is

$$\dot{x} = f(x) + B_2 u + B_1 \dot{w} + \text{gravity} \tag{1.3}$$

where,

$$f(x) = \begin{bmatrix} 0 & 0 & -x_3 & 0 \\ 0 & 0 & 0 & -x_4 \\ \frac{K}{M}x_1 & -\frac{K}{M}x_2 & -\frac{C}{M}x_3 & \frac{C}{M}x_4 \\ -\frac{K}{M}x_1 & \frac{K+K_t(x_2)}{m}x_2 & \frac{C}{m}x_3 & \frac{C+C_t(x_2)}{m}x_4 \end{bmatrix} \tag{1.4}$$

$$B_2 = [\ 0; 0; 1/M, -1/m\ ] \tag{1.5}$$

$$B_1 = [\ +1, +1, 0, C_t(x2)/m\ ]' \tag{1.6}$$

where $K_t(x_2)$ is the instantaneous value of the tire stiffness coefficient, i.e., $K_t(x_2) = f_k/x_2$, B_2 and B_1 are the control and disturbance input matrices, respectively, and, $\dot{w}$ the rate of change of road unevenness, is the disturbance input (process noise). Since the displacement states are measured from the unloaded springs references (not the static equilibrium references) 'gravity' is included in the equations of motion to account for the contributions of weights of the sprung and unsprung masses. The last row of f(x),

Equation 1.4, and the last row of B_1, Equation 1.6, are the nonlinear terms associated with the tire in this state variable formulation. A notable observation is that these nonlinearities are only functions of x_2. The other nonlinearities, i.e., the separation of the tire from the road and exhaustion of the suspension travel are considered as variation of the model structure.

The nonlinear state variable formulation of Equation 1.3 can be replaced by a set of linear state space representations, using the two methods of: 1) linearizing around a set of operating points and 2) substituting the nonlinear terms $K_t(x_2)$ and $C_t(x_2)$ by constants evaluated at a predefined set of x_2's. Both approaches result in an array of linear models. Considering the fact that more accurate tire behaviour (in terms of K_t and C_t) are normally in the form of look-up tables, the latter is a more convenient approach and is taken in this work. Using the notion of fuzzy (multivariance) logic, the instantanious nonlinear suspension model is described by all these linear models, simultaneously, only to varying degrees.

Considering the two elements of $a = [C_t(x_2)\ K_t(x_2)]$ as uncertain parameters which can assume a set of possible values (depending on the tire deflection x_2), a collection of linear models are developed by dividing the range of tire deflection into J discrete regions, x_{2j} (j = 1,2,.....J), and considering C_t and K_t as constants, evaluated at the centroid of these regions. The dynamic declaration of the instantaneous linear model, most closely representing the nonlinear system, is based on estimation of x_2 using a bank of state estimators.

State space representation of the j-th system is

$$\dot{x} = A_j x + B_2 u + B_{1j} w \tag{1.7}$$

$$y = Cx + D_2 u + D_1 w + v \tag{1.8}$$

$$A = \begin{bmatrix} 0 & 0 & -1 & 0 \\ 0 & 0 & 0 & -1 \\ \frac{K}{M} & -\frac{K}{M} & -\frac{C}{M} & \frac{C}{M_4} \\ -\frac{K}{M} & \frac{K + K_t(x_2 j)}{m} & \frac{C}{m} & \frac{C + C_t(x_2 j)}{m_4} \end{bmatrix} \tag{1.9}$$

$$B_2 = [\ 0; 0; 1/M, -1/m\ ] \tag{1.10}$$

$$B_{1j} = [\ +1, +1, 0, C_t(x2)/m\ ]' \tag{1.11}$$

where j = 1,2,...., J and w and v are disturbance and measurement noise inputs assumed to be uncorrelated, zero-mean, white, Gaussian processes with auto-correlations of W and V respectively, i.e.,

$$E\{ w(t)\ w(\tau)' \} = w\ \delta(t - \tau) \tag{1.12}$$

$$E\{ v(t)\ v(\tau)' \} = v\ \delta(t - \tau) \tag{1.13}$$

where E{.} denotes the expectation operator, and $\delta(.)$ is the Dirac delta function. Using the measurement of the displacement between the sprung and the unsprung masses as the output yields

$$C = [+1 \quad -1 \quad 0 \quad 0] \tag{1.14}$$

$$D_2 = [0] \tag{1.15}$$

$$D_1 = [0] \tag{1.16}$$

However, if the sprung mass acceleration is considered as the output, then C, D_2 and D_1 matrices will be the entries of the third row of A_j, B_2 and B_{1j} matrices (Equations 1.9, 1.10 and 1.11) of the state equation.

The actuation force measured by the load cell is one of the inputs to all the estimators in the bank.

Active suspension can be grouped into two major categories: fully active suspension and semi-active suspension. In the first type, the sprung and unsprung masses namely the body and the wheel base, are only connected by an actuator, as seen in Figure 1.3. Characteristic for the semi-active case is that there is a passive element (spring) or a combination of passive elements (spring and dashpot) in parallel to the active element. In [28] this case is further categorized into fast (Figure 1.4) and slow (Figure 1.5) semi active suspension. The latter has, in addition to the passive element in parallel to the actuator, also a passive element in series with the active one. In [28] it is claimed that it is possible to achieve better performance results using slow active suspension unlike in [36] this configuration is blamed not to be failure safe in experiments. Because of this problem and also due to the fact that all other authors except those of [28] use the setup shown in Figure 1.4, it is used in this work. The fully active case is not chosen due to its high power consumption.

Without a spring in parallel to the actuator, the actuator has to support the car body mass, due to this it consumes a lot of energy. The actuators are subject to two different operating conditions, when the road disturbance on the suspension is small (smooth road), the actuators are under relatively high load (weight of the vehicle), but are displaced at a very low rate, an ideal condition for high pressure-regulated valve-controlled systems. However, the requirement on the active suspension system to react to road disturbance effectively makes the actuator subject to high displacement rates, which in turn requires high flow rate on the hydraulic fluid. Therefore, a hydraulic system for

the active suspension without a passive element, would be a high flow-rate pressure-regulated valve controlled system. Such systems convert a large rate of hydraulic system energy to heat at regulating valves, which is not desirable.

As the so called fully active suspension has limited practical use, most authors use a different terminology than that of [28]. The fast semi-active suspension is referred to as active suspension, and the term "semi-active suspension" is one having a passive element with variable damping or variable stiffness but without an active element. In this work the configuration in Figure 1.4 is called the active suspension.

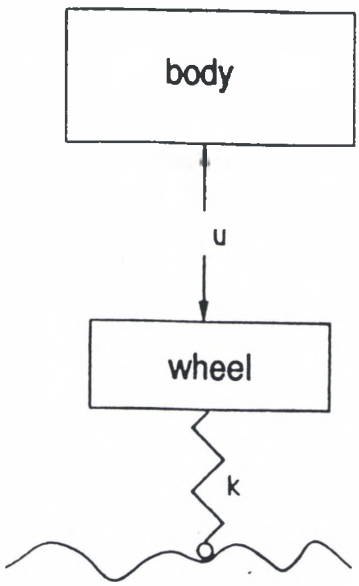

Figure 1.3 - Fully Active Suspension

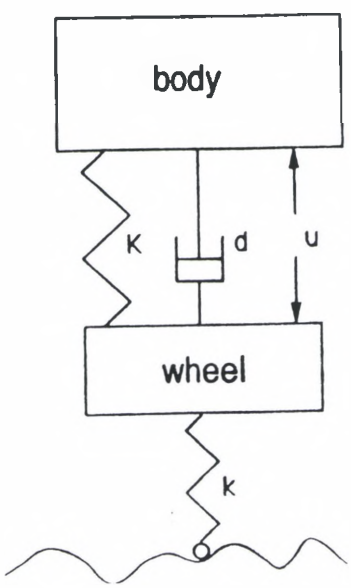

Figure 1.4 - Fast Semi-Active Suspension

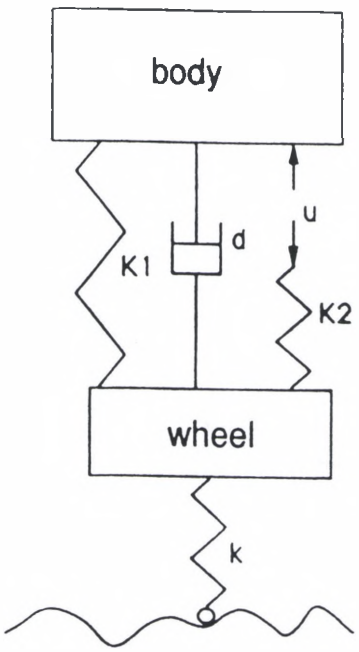

Figure 1.5 - Slow Semi-Active Suspension

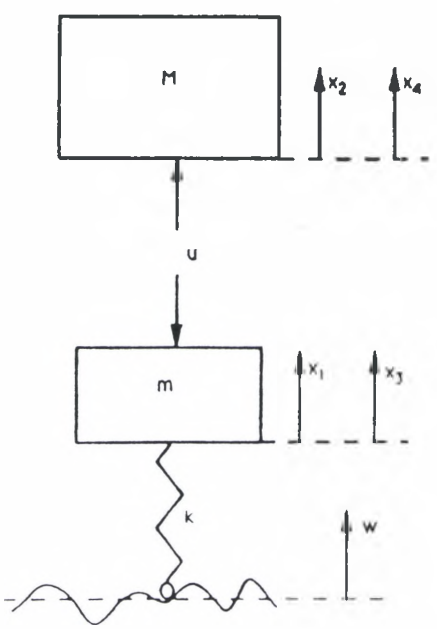

Figure 1.6 - Possible State Space Representation of the Quarter Car Model

State of the Art in Active Suspension Design

To improve road contact and comfort there are two major concepts to design the controller for the active element. The first is to use the optimal control theory (time domain approach), the second is the shaping of the velocity transmissibilities (frequency domain approach). In the following, only 2-DOF systems are discussed, because 1-DOF systems, used in some publications, omits wheel base and tire which changes the nature of the system.

Optimal Control

Linear Quadratic Regulator (LQR)

The emphasis of optimal control theory is to minimize the objective function given by,

$$J = \int_0^\infty (xQx' + uRu')dt \qquad (1.17)$$

where x is the state vector and u is the control force. Q, R and N are weighting matrices constrained to Q being a positive semi-definite symmetric, R being a positive definite symmetric, and (Q- $N' R^{-1} N$) being a positive semi-definite matrix. Minimizing this integral implies minimizing the area under the squared trajectories of x and u when the controller drives the system back to zero from a non-zero initial condition. In the case of automotive suspension, the crucial values are the peak values of discomfort and wheel load variation in response to road disturbance, e.g. a bump or a pothole. The peak value of body acceleration describes the passenger discomfort whereas the peak value of loss of road contact determines vehicle performance and stability. The motivation for using optimal control techniques (LQR) for active suspensions is due to the fact that the peak

values so obtained tend to be smaller than the passive suspension system for most disturbance input responses.

The importance of using LQR is partly due to the existence of a closed form solution for the minimization of Equation 1.17. If the upper bound is not infinity, minimization of the above equation leads to the following matrix differential equation:

$$A' S + S A + S B R^{-1} B' S + Q = \dot{S} \tag{1.18}$$

with the control law

$$u(t) = -F x(t) \tag{1.19}$$

is calculated by

$$F = R^{-1} A' S$$

with A and B represented by state space,

$$\dot{x} = A x + B u \tag{1.20}$$

In the steady state, i.e. the upper bound of the integral is infinity, the differential Equation 1.18 results in a algebraic Riccati equation:

$$A' S + S A + S B R^{-1} B' S + S = 0 \tag{1.21}$$

This can be represented in a generic form as

$$J = \int_0^{\infty} \begin{bmatrix} x' & u' \end{bmatrix} \begin{bmatrix} Q & N \\ N' & R \end{bmatrix} \begin{bmatrix} x \\ u \end{bmatrix} dt \tag{1.22}$$

An LQR optimal controller not only finds the optimal control law by minimizing Equation 1.17, but also guarantees infinite gain and phase margins of atleast 60 degrees for the closed loop system.

As mentioned earlier, first attempts were made in the late sixties and early seventies to apply active supension system control in automobiles. The easiest model so

chosen, namely the quarter car suspension model has 4 states. The early attempts applying optimal control suffer lack of straight-forward choice of the weights Q and R to match performance objectives, i.e. comfort and road contact. This gap is closed in the publications of the eighties, dealing with optimal control which focus on a proper choice for Q and R and the problem of not having access to all the states, which complicates the use of full state feedback technique such as LQR. One of the first suggestions were made by Thompson, 1984 [31]. He suggested a structure of R, which yields a cost function containing the control force, working space and road contact. Note that the incorporation of road contact makes a special kind of state space representation necessary based on Figure 1.6. The states are absolute displacement, i.e. displacement not relative to the ground (road surface), velocity of the body and absolute displacement and velocity of the wheel base. The state space representation is

$$\dot{x} = A\,x + B\,u + G\,w$$

$$y = C\,x \tag{1.23}$$

where,

$$A = \begin{bmatrix} 0 & 0 & 1 & 0 \\ 0 & 0 & 0 & 1 \\ -\frac{K}{m} & 0 & 0 & 0 \\ 0 & 0 & 0 & 0 \end{bmatrix} \tag{1.24}$$

$$B = [\ 0;\ 0;\ -1/m;\ 1/M],$$

$$G = [\ 0;\ 0;\ k/m;\ 0]$$

where u is the control force input, and w is the input of the road surface variation (disturbance input). Recall that M is the mass of the body, m the mass of the wheel base, K the stiffness of the spring in the suspension unit, C the damping coefficient of the dashpot, K_t the tire stiffness and C_t the tire damping coefficient.

Inclusion of the working space, road contact and control force in the objective funciton yields

$$J = \int_0^\infty (\text{rho1}(w - x_2)^2 + \text{rho2}(x_1 - x_2)^2 + \text{rho3}u^2)dt \qquad (1.25)$$

with rho1, rho2 and rho3 being the weights on road contact ($w-x_2$), working space (x_1-x_2) and control force respectively.

The representation in Equation 1.25 considers only absolute values of displacement and velocity of the body. It can be transformed to Equation 1.26 which considers relative values of displacement and velocity of the body, hence another state space representation is needed as shown in Figure 1.7. The states are the relative displacements between the road surface and the body and between road surface and wheel base and the velocities of the body and the wheel base. It is important to note that the disturbance input is no longer the variation of road surface, but its derivative. The Equations 1.23 and 1.24 can be replaced by the following

$$x_1 = w - x_1$$

$$x_2 = w - x_2 \qquad (1.26)$$

yields $$\dot{x} = A x + B u + G w \text{ and } y = Cx \qquad (1.27)$$

with $$A = \begin{bmatrix} 0 & 0 & 1 & 0 \\ 0 & 0 & 0 & 1 \\ -\frac{K}{m} & 0 & 0 & 0 \\ 0 & 0 & 0 & 0 \end{bmatrix} \qquad (1.28)$$

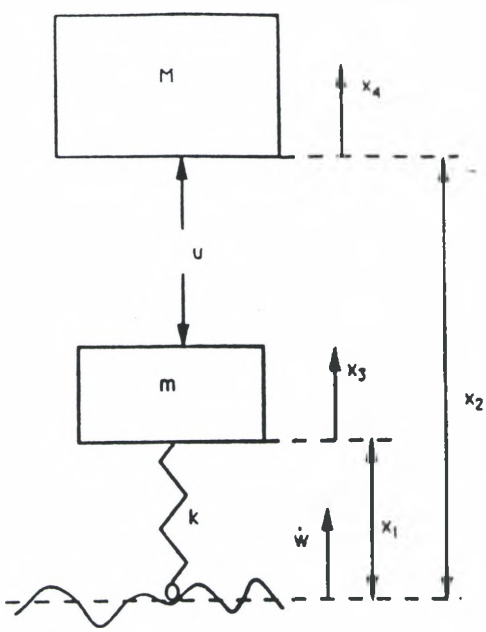

Figure 1.7 - Alternative State Space Representation of the Quarter Car Model

B = [0; 0; -1/m; 1/M],

G = [-1; -1; 0; 0]

The new cost function is

$$J = \int_0^{\infty} (\text{rho1}x_2^2 + \text{rho2}(x_1 - x_2)^2 + \text{rho3}u^2)dt \tag{1.29}$$

which is the the same as Equation (1.1) with

$$A = \begin{bmatrix} \text{rho1} + \text{rho2} & -\text{rho2} & 0 & 0 \\ \text{rho2} & \text{rho2} & 0 & 0 \\ 0 & 0 & 0 & 0 \\ 0 & 0 & 0 & 0 \end{bmatrix} \tag{1.30}$$

R = rho3

This objective function now takes into consideration the road contact and the working space. The distance variation between the road surface and the body and between the road surface and the wheel base are not accessible. Hence Thompson [32] first suggested the use of radar and sonar devices to measure the distance between the body and the road surface with some practical difficulties, using these devices. The distance between the body and the wheel base and accelerations of both the body and the wheel base are accessible measurements unlike the velocity and absolute displacements, which aren't directly accessible but can be obtained by subsequent integration of the accelerations. This method would result in inaccurate measurements due to integration offset and is therefore neglected. The second suggestion [31], avoided the need for sensoring the relative displacement of sprung mass which resulted in a reduced cost function referred to as the suboptimal control. This cost function contains the working space and the control force but not the road contact which makes it possible to use the

state space representation in Equations 1.22 and 1.23. For certain cases, it was observed that the control obtained by this method was very slightly inferior to that of optimal control, though in general, the optimal technique is far superior to that of the suboptimal one. The suboptimal objective function contained neither the road contact nor the comfort, hence Q has to be obtained by trial and error. For this system, the LQR technique can be applied and a full state feedback vector, **feed**, can be found.

The control law is given by $u = - feed * x$ (1.31)

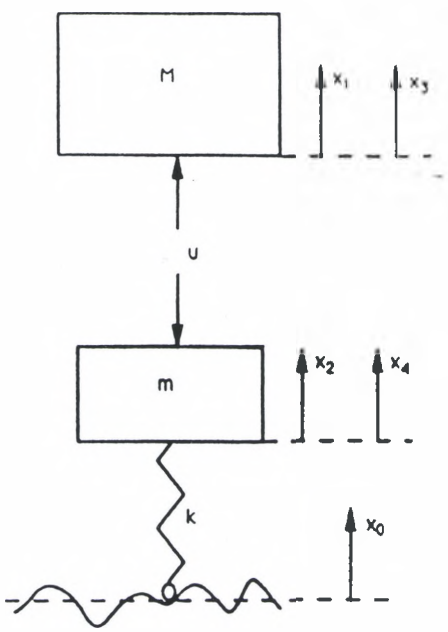

Figure 1.8 - State Space Representation chosen by Wilson et al

Like in [35], road contact is included by Hac in ([10] and [11]). However, the use of disturbance dynamics to avoid road contact as a state is just a side effect. Hac makes use of another interpretation of the LQR technique. It can be viewed as a controller minimizing the auto-correlation of the states with respect to a white noise disturbance input [10]. He replaced the algebraic Riccati equation incorporating the uncontrollable dynamics by a set of equations: an algebraic Riccati equation with only controllable dynamics, two linear matrix equations and a Lyapunov equation.

In his work, active suspension was used having a spring and a dashpot in parallel with the active element. The states x_1 and x_2 were defined as the absolute displacements of the sprung and the unsprung masses and x_3 and x_4 being the velocities of sprung and unsprung masses respectively. The objective function contains the discomfort, wheel load variation, working space and control force, which yields the general form of a cost function of the type in Equation 1.22. The state space representation is given by

$$\dot{x} = A\,x + B\,u + G\,\dot{w} \tag{1.32}$$

with

$$x = [x_s, x_w] \tag{1.33}$$

where xs and xw are the states of the quarter car model and the disturbance. The full state feedback matrix **feed** of the control law is

$$F = R^{-1}(N' + B'S) \tag{1.34}$$

with 'S' being the solution of the algebraic Riccati equation

$$S(A - B\,R^{-1}N') + (A - B\,R^{-1}N')'S - S\,B\,R^{-1}B'S + (Q - N\,R^{-1}N') = 0 \tag{1.35}$$

Equation 1.35 has no solution due to the uncontrollable poles in the disturbance dynamics. Therefore Hac suggests a partioning of Q and S.

$$Q = \begin{bmatrix} Q_{xx} & Q_{xw} \\ Q_{wx} & Q_{ww} \end{bmatrix}$$

(1.36)

$$S = \begin{bmatrix} S_{xx} & S_{xw} \\ S'_{wx} & S_{ww} \end{bmatrix}$$

The dimensions of Q_{xx} and S_{xx} correspond to the number of controllable dynamics of the system and the dimensions of Q_{ww} and S_{ww} to the number of uncontrollable dynamics resulting from the disturbance. After certain manipulations, the following set of equations are obtained instead of Equation 1.35.

$$S_{XX} (A_x - B_x R^{-1} N_x') + (A_x - B_x R^{-1} N_x')' S_{xx} - S_{xx} B_x R^{-1} B_x' S_{xx} + (Q_{xx} - N_x R^{-1} N_x') = 0 \quad (1.37)$$

$$S_{xw} A_w + ((A_x - B_x R^{-1} N_x')' - S_{xx} B_x R^{-1} B_x')S_{xw} + S_{xx} B_x + Q_{xw} = 0 \quad (1.38)$$

$$A_w' S'_{xw} + S'_{xw}((A_x - B_x R^{-1} N_x')' - B_x R^{-1} B_x' S_{xx}) + B_x' S_{xx} + Q'_{xw} = 0 \quad (1.39)$$

$$S_{ww} A_w + A_w' S_{ww} + (S'_{xw} B_x + B_x' S_{xw} + Q_{ww} + S'_{xw} B_x R' B_x' S_{xw}) = 0 \quad (1.40)$$

Then the feedback law is

$$u = - \mathbf{feed}' \, x_s \quad (1.41)$$

where **feed'** is calculated by

$$\mathbf{feed}' = R^{-1} ((N_x' + B_x' S_{xx}) B_x' S_{xw}) \quad (1.42)$$

The single subscript x indicates system matrices corresponding to the quarter car model described by the state vector 'x_s' and the single subscript 'w' is used for matrices corresponding to the disturbances described by the state vector x_w. Equations (1.37 - 1.40) can be solved consecutively, however, only Equations 1.37 and 1.38 are necessary to solve for **feed** in Equation 1.42. Hac reports good results under the assumption that the states are accessible whereas in reality they are not, hence an observer would be necessary to implement the controller.

Linear Quadratic Gaussian (LQG)

The main drawback of the LQR technique is that the measurement of all the states are required to be fed back. In most of the cases not all the states are measurable, hence they have to be estimated. The most advanced technique for state estimation is still the Kalman-Bucy-Filter. This filter is a model of the original plant, namely the quarter car suspension model, to simulate the states and an injection matrix **H** through which the error between actual plant output and model output is fed back into the model. The crucial part is the choice of **H**, since, if it approaches infinity (Leonhard observer), the estimation becomes very tight, sensor noise is also amplified with an infinite gain, resulting in sensor noise driving the estimator. If **H** is too small, the estimation becomes inaccurate due to the plant disturbance and uncertainities of the plant model. The Kalman-Bucy-Filter provides an optimal trade-off between plant disturbance noise and sensor noise.

The filter state space representation is given by

$$\dot{x} = A x + B u + G w \tag{1.43}$$

$$y = Cx + v$$

with w(t) and v(t) being the white Gaussian noise and

$$E\{ \dot{w}(t)\ \dot{w}(\tau)\} = w\ \delta(t - \tau) \qquad (1.44)$$

$$E\{v(t)\ v(\tau)\} = v\ \delta(t - \tau)$$

The solution of the injection matrix **H** results from the solution of the following algebraic Riccati equation

$$S A' + A S - S C' v^{-1} C S + G w G' = 0 \qquad (1.45)$$

and

$$H = v^{-1} C S \qquad (1.46)$$

In the LQR technique all the states are fed back whereas in the LQG case, the estimated states (using the Kalman-Bucy-Filter for state estimation) are fed back. The weakness of this technique is that it lacks the excellent robustness properties possessed by LQR.

Classical Suspension Design

This method involves shaping of the frequency responses of the transfer functions of the velocity of wheel base over the velocity of disturbance input and the velocity of the body over the velocity of disturbance input. These transfer functions are called transmissibilities. The use of LQR is a general approach coming from the controls point of view and is applied in the case of a suspension system. Transmissibility shaping, however, is the traditional design originating from the passive suspension system. The objective of the design is to minimize the discomfort and wheel load variation respectively.

An ideal system is a system with only (fictional) skyhook damping (see Figure 1.14) with

$$E_1 = E_2 = 0.7 \tag{1.47}$$

where,

$$E_1 = (d_1/2)\, M\, w_1$$

$$E_2 = (d_2/2)\, M\, w_2 \tag{1.48}$$

and

$$w_1 = \sqrt{K / M}$$

$$w_2 = \sqrt{k / m} \tag{1.49}$$

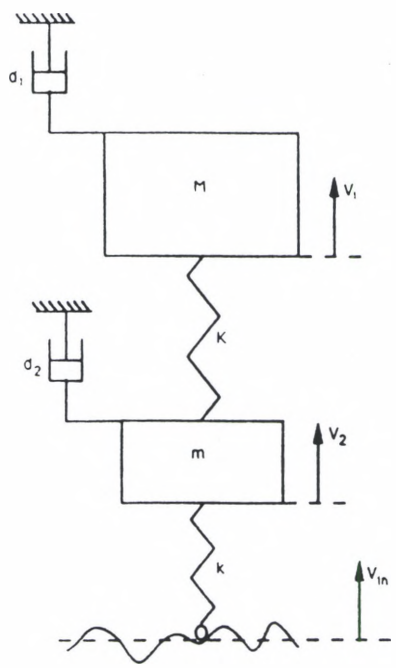

Figure 1.9 - Ideal Suspension

This is considered an excellent suspension system since the sprung mass (M) resonance is controlled, coupled with the excellent high frequency isolation. The wheel motion exhibits perfect tracking of the road, i.e. $v_2/v_{in} = 1$, over a broad frequency range with no tendency to leave the ground at high frequencies [23]. The goal of active suspension design is to find a control law for the active element, such that the shape of the transmissibilities approaches the behaviour of the transmissibilities for the fictional skyhook system as closely as possible.

As found in literature, to obtain transmissibilities similar to that of a fictional skyhook suspension, the coefficients of the transfer functions of the ideal system's transmissibilities are matched using full state feedback, or limited full state feedback as suggested in the earlier literature.

CHAPTER II

CONTROL DESIGN

The State Space Model

Linear Quadratic Gaussian technique is an LQ full state feedback controller which uses the error covariance optimal estimate of the states, provided by a Kalman filter, in place of measured states.

The primary objective of each controller gain block in Figure 2.0 is to minimize the quadratic cost function

$$J = \int_0^{\infty} \begin{bmatrix} x' & u' \end{bmatrix} \begin{bmatrix} Q & N \\ N' & R \end{bmatrix} \begin{bmatrix} x \\ u \end{bmatrix} dt \qquad (2.1)$$

with Q, R and N being the same as explained in the previous chapter.

The design of each Kalman filter and gain matrix is based on a particular value of the parameter vector aj. Minimizing the absorbed power (related to frequency weighted time integral of the sprung mass squared acceleration) is the main objective of the LQ controller. To accomodate this objective, the sprung mass acceleration is filtered by an experimentally derived, 6 th order, frequency dependent weighting function depicting the human body's tolerance to vibration (Lins, 1972), and included in the objective function. Figure 2.1(a) compares the frequency responses of the original 6th order filter with its 2nd order approximation. The use of the low-order filter of Equation 2.2 results in an

augmented system with 6 states (4 from the original suspension and 2 from the filter) and avoids having excessive number of states.

$$F(s)=\frac{12s}{s^2+30.02s+901.3} \tag{2.2}$$

The filter equations can be represented by:

$$\dot{x}_f = A_f x_f + B_f u_f \tag{2.3}$$

$$y_f = C_f x_f \tag{2.4}$$

Rattlespace, tire deflection and control force are also included in the objective function to assure that minimizing the absorbed power (discomfort) is not achieved at the expense of excessive suspension travel, tire deflection and control as seen in Equation 2.5.

$$J = \int_0^\infty (rho4(\dot{x}_3 f)^2 rho1 x_2^2 + rho2(x_1 - x_2)^2 + rho3u^2)dt \tag{2.5}$$

where $\dot{x}_3 f$ is the filtered sprung mass acceleration, rho 1, rho 2, rho 3 and rho 4 are the weights on tire deflection (road contact), working space, control force and filtered body acceleration, respectively. Note that one rho i can be set to constant and the remaining are chosen relative to the one set. In this work rho 4 is set to 1. The objective function is augmented with the frequency weighted human body response filter at the sprung mass acceleration output as can be seen from Figure 2.1 (b)

Equation 2.5 can be written in the form of Equation 2.1, using the following Q, R and N:

$$Q = \begin{bmatrix} \frac{K^2}{M^2} + rho1 & -\frac{K^2}{M^2} - rho1 & \frac{CK}{M^2} & -\frac{CK}{M^2} \\ -\frac{K^2}{M^2} - rho1 & -\frac{K^2}{M^2} + rho1 + rho2 & -\frac{CK}{M^2} & \frac{CK}{M^2} \\ \frac{CK}{M^2} & -\frac{CK}{M^2} & \frac{C^2}{M^2} & -\frac{C^2}{M^2} \\ -\frac{CK}{M^2} & \frac{CK}{M^2} & -\frac{C^2}{M^2} & \frac{C^2}{M^2} \end{bmatrix} - \frac{CK}{M^2} \qquad (2.6)$$

$$R = [-\frac{1}{M^2} + rho3] \qquad (2.7)$$

$$N = [\frac{K}{M^2} - \frac{K}{M^2}\frac{C}{M^2} - \frac{C}{M^2}] \qquad (2.8)$$

Combining the two state space realizations of the suspension (Equations 1.7 and 1.8) and the filter (Equations 2.3 and 2.4), the augmented state space realization can be seen in Equations 2.6 and 2.7; see also Figure 2.1 (b).

$$\begin{bmatrix} \dot{x} \\ \dot{x}_f \end{bmatrix} = \begin{bmatrix} A_j & 0 \\ B_f C & A_f \end{bmatrix} \begin{bmatrix} x \\ x_f \end{bmatrix} \begin{bmatrix} B_2 \\ B_f D_2 \end{bmatrix} u + \begin{bmatrix} B_{1_j} \\ B_f D_1 \end{bmatrix} w \qquad (2.9)$$

From Equation 2.4, it can be seen that the output of the filter has a strictly rational transfer function (no D_f term), when the sprung mass acceleration is viewed as the output, its augmentation with the suspension model will still yield a strictly rational overall transfer function. That is, the D term in the output, Equation 2.7, of the augmented system, representing the filtered sprung mass acceleration, is zero matrix.

$$y = \begin{bmatrix} 0 & C_f \end{bmatrix} \begin{bmatrix} x \\ x_f \end{bmatrix} \qquad (2.10)$$

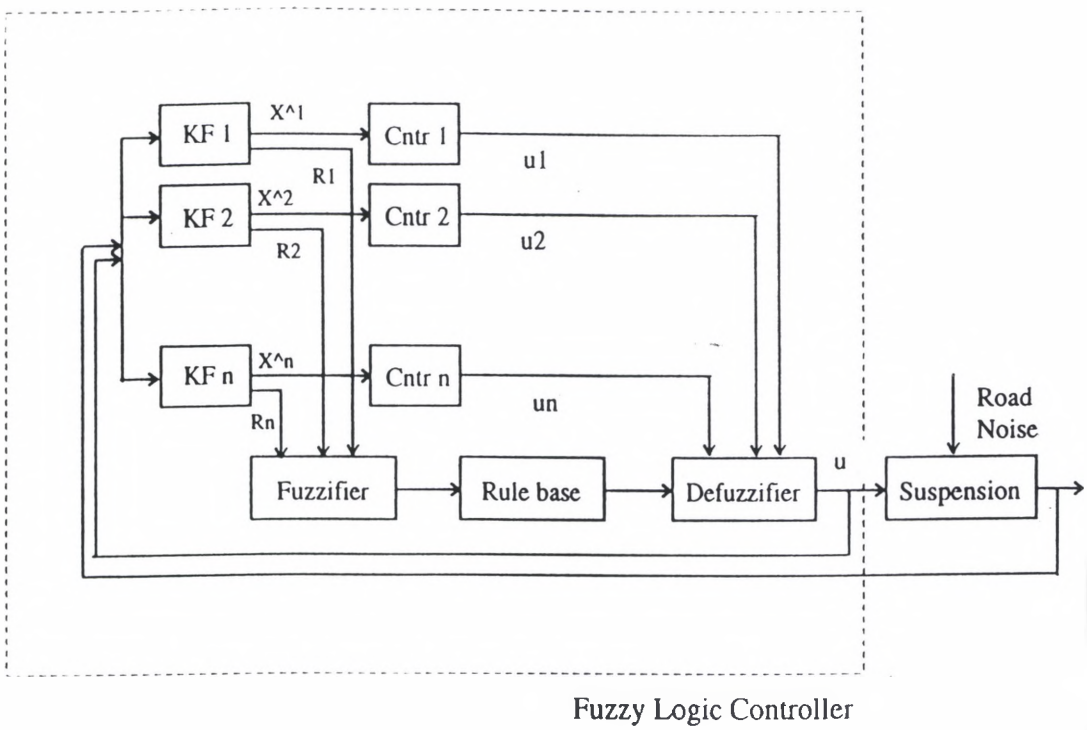

Figure 2.1 (a) - Structure of the Fuzzy Logic Suspension Controller

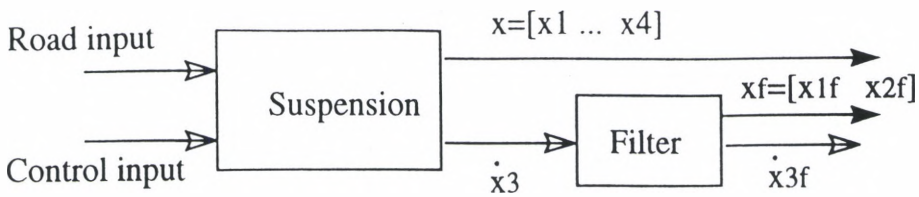

(b) Augmented Suspension

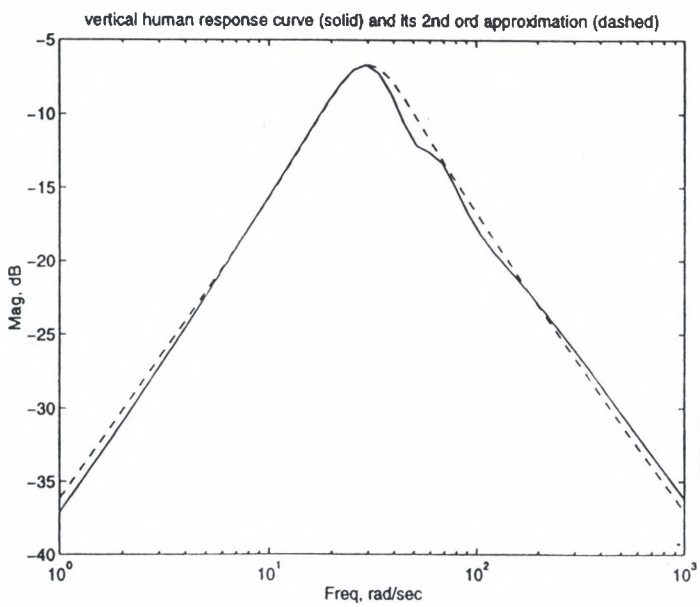

(c) Human Body Response Filter and its Second Order Approximation

It should be noted that in this case the weights rho 1, rho 2 and rho 3 cannot be chosen independently because $\mathbf{Q - N' R^{-1} N}$ has to be positive semi-definite. In LQG, the estimator gains are designed in a manner to provide a trade-off between the necessity of a tight estimation due to the disturbances perturbing the plant and the necessity of a loose estimation due to the noise corrupting the measurement.

Since the ratio w/v, not w and v independently, has influence on the estimator gains, one of them is set to one and the other varied. It turns out that a reasonably high w, however results in a practically unstable system. For w of higher than 1e8 which is a necessary condition for good performance, the system has a gain margin of about 0 db and a phase margin of 0 degrees. A very small perturbation, e.g. change in parameters, would make the system unstable. This suggests that LQG is not an appropriate technique for active suspension systems. Low stability robustness of LQG is the main reason for its lack of widespread acceptance among practitioners, especially in areas like flight control and chemical processes control in which stability robustness is a sensitive issue.

Equation 2.5 can be written as Equation 2.1, using the appropriate Q, R and N; [15]. The zero D matrix in the output (filtered acceleration), Equation 2.7 indicates that N, the cross term in the objective function, is a zero matrix. Knowing Q and R matrices, the full state feedback gain vector, $\mathbf{KK = [\ feed \quad k_f]}$ is evaluated by solving the appropriate Riccati equation. The state feedback control law for the augmented system is obtained by standard methods to yield the control force of Equation 2.8.

$$u = \text{feed}\, x + k_f x_f \tag{2.11}$$

The effect of variation in the weighting factors (rho i's) on the absorbed power, mean squared filtered sprung mass acceleration surface (representing the absorbed power)

in response to 1.35" Letourneau course, traversed at 25 mph, road velocity input is evaluated and presented in Figure 2.3. This is done using one of the elements of the set of linear models describing the non linear suspension. As expected, lowering the weight on control input rho 3, i.e., willing to spend high control energy, in conjunction with a small weight on road contact (tire deflection), lowers the absorbed power.

The effectiveness of the frequency-shaped design in lowering the sprung mass acceleration at the frequency range of importance in human body power absorption, is depicted in Figure 2.2 in which two different control designs are compared. These designs are based on having the sprung mass acceleration $\dot{x}_3$ or filtered sprung mass acceleration $\dot{x}_3 f$ in the objective function of Equation 2.5 with the same set of weights for both designs. Frequency shaped design gives a significant improvement over the non-frequency-shaped design.

The addition of 2 states to the plant resulting from augmenting the plant with the human body response filter of Equation 2.2 does not add any extra computational burden to the real-time estimation of the states. This is because, the two states of the filter can be accurately measured by running the measured acceleration of the sprung mass through an op-amp based electrical circuit realizing the filter. This will leave the estimation based on the original 4 states of the suspension itself.

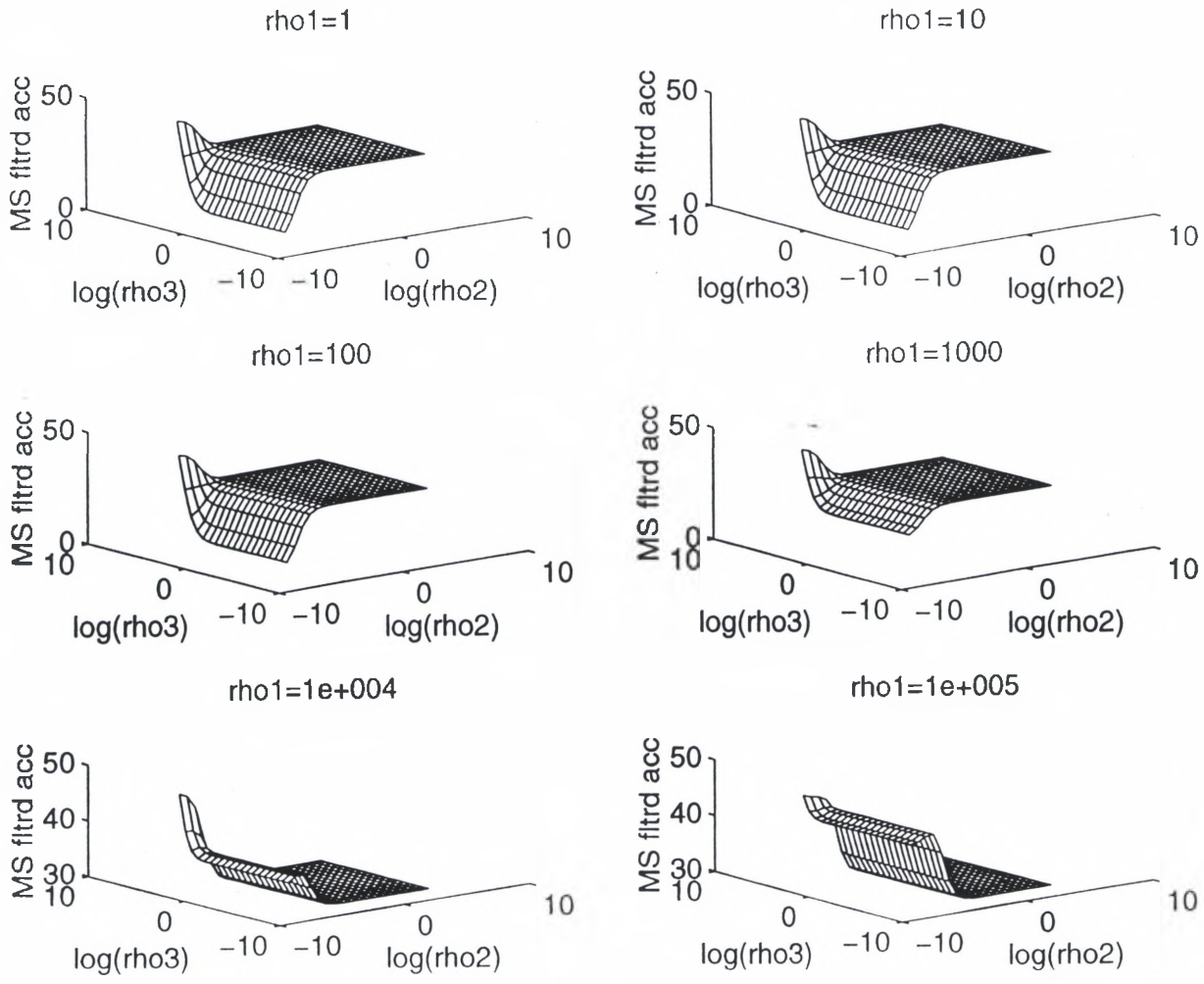

Figure 2.2 - Mean Squared Filtered Sprung Mass Acceleration Surface for various weights

The following steps are taken to avoid inclusion of servohydraulics dynamics in the estimators and controllers design: 1) The measured (not calculated) control force (control input) is fed to the real-time estimation routines. This is possible because the actuator is equipped with a load cell. And 2) By closing a feedback innerloop around the actuator force the servohydraulics bandwidth is widened, eliminating the need for inclusion of its dynamics in the controller design. Figure 2.3 shows the effectiveness of a proportional plus integral (PI) inner loop force controller in eliminating the dynamics of the hydraulic system.

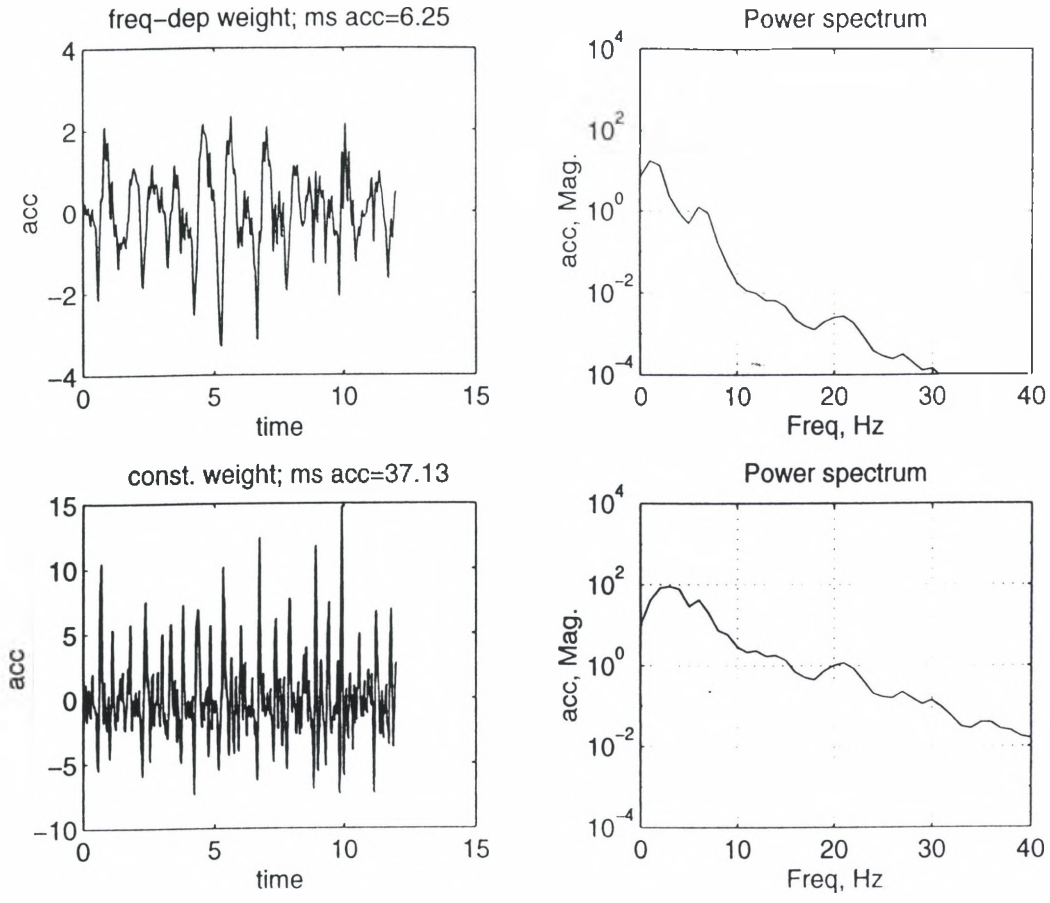

Figure 2.3 - Time and Frequency Responses of the sprung mass acceleration with frequency and non-frequency shaped controllers

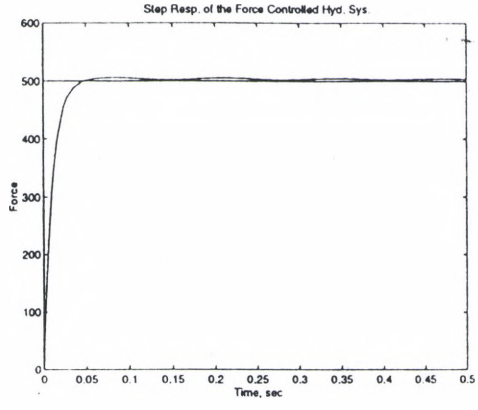

Figure 2.4 - Response of closed-loop force controlled hydraulic system to step reference force

Multiple Model Based Estimated States

Multiple model Kalman filter-based estimation consists of a bank of J separate estimators, each based on a particular value of the vector of uncertain parameters, $a = [k_t \; c_t]^*$, i.e., $a_1, a_2, ..., a_j$. The use of filter banks running in parallel was first suggested by Magill [23]. The Baysian conditional probability was used in the scheme proposed by Magill to estimate the states as the conditional mean of the estimated states by all the filters in the bank. Although the use of a bank of Kalman filters was considered impractical at the time it was proposed, recently with the advances in digital signal processing computer technology, on-line implementation of this scheme is quite feasible and has been demonstrated in a number of applications.

The Baysian conditional minimum mean square error estimate of the state is the probability weighted average:

$$\hat{x}(t_i^+) = E\{x(t_i) \mid Z(t_i) = Z_i\}$$

$$= \sum_{j=1}^{J} (\hat{x}_j(t_i^+).\, P_j(t_i)) \qquad (2.12)$$

where $Z(t_i)$ is the measured output history vector, Z_i is the realized output history vector, $\hat{x}_j(t_i^+)$ is the state estimate generated by the j^{th} Kalman filter based on the assumption that parameter vector is equal to a_j and $p_j(t_i)$ is the conditional Gaussian probability of that event, i.e., $a = a_j$, occuring.

The evaluation of $p_j(t)$ is based on certain assumptions which might not always be valid. Moreover, fuzziness not probability, is the right approach for estimating the states by blending the estimates of individual Kalman filters. This is because probability describes the uncertainity of event occurance (whether it occurs) not the degree to which

an event occurs (which is described by fuzziness). In other words whether an event occurs is random, to what degree it occurs is fuzzy. The method proposed by Magill serves as a good point of departure for fuzzy logic estimation of states, as to be described in Appendix A.

CHAPTER III

KALMAN ESTIMATOR

Filter Theory

The purpose of the Linear Quadratic Control technique is to estimate the states from the output of the quarter car suspension model, which can then be used to calculate the control force. This estimation is done by a Kalman filter based on the assumption that the parameter vector equals aj, since each filter is based on a particular value of the vector of uncertain parameters, **a**, in a given linear stochastic state model for a dynamic system. In order to make simultaneous estimation of states and parameters tractable, the continuous range of the parameter values is discretized into j representative values More explicitly, let the model corresponding to aj be described by an "equivalent discrete-time model" [26] for a continuous-time system with sampled data measurements:

$$x_j(t+1) = \varphi_j\{t_{i+1}, t_i\}\, x_j(t_i) + G_{2j}(t_i)\, u(t_i) + G_{1j}(t_i)\, w_j(t_i) \quad (3.1)$$

$$y(t_i) = C_j(t_i)\, x_j(t_i) + v_j(t_i) \quad (3.2)$$

where, φ_j is the state transition matrix, $[G_1\ G_2]_j$ is the input matrix, x_j is the state, u is the control input, w_j is the discrete time zero mean white Gaussian dynamics noise of covariance $Q_k(t_i)$ at each t_i, z is the measurement vector and v_j is discrete time zero mean white Gaussian measurement noise of covariance $R_k(t_i)$ at t_i, assumed independent of w_j; $x(t_0)$ is modelled as Gaussian, with mean $\hat{x}_j(t_0)$ and covariance P_{j0}, assumed independent

of w_j and v_j.

Based on this model the Kalman filter is specified by the Measurement Update:

Filter covariance,

$$F_j(t_i) = C_j(t_i)\, P_j(t_i^*)\, C_j'(t_i) + v_j(t_i); \quad (3.3)$$

Kalman gain,

$$L_j(t_i) = P_j(t_i^*)\, C_j'(t_i)\, F_j'(t_i); \quad (3.4)$$

State Estimates,

$$\hat{x}_{jj}(t_i) = \hat{x}_{jj}(t_i^*) + L_j(t_i)[y(t_i) - C_j(t_i)\, \hat{x}_{jj}(t_i^*)] \quad (3.5)$$

Error Covariance,

$$P_j(t_i) = P_j(t_i^*) - L_j(t_i)\, C_j(t_i)\, P_j(t_i^*); \quad (3.6)$$

The Kalman filter updates the above estimation by the effects of process and measurement noises.

And the Propagation Relation:

State Estimates,

$$\hat{x}_{jj}(t_{i+1}^*) = \varphi_j\{t_{i+1}, t_i\}\, \hat{x}_{jj}(t_i+) + G_{2j}(t_i)\, u(t_i) \quad (3.7)$$

Error Covariance,

$$P_j(t_{i+1}^*) = \varphi_j\{t_{i+1}, t_i\}\, P_j(t_i^+)\, \varphi'_j(t_{i+1}), t_i) + G_{1j}(t_i)\, w_j(t_i)\, G_{1j}'(t_i) \quad (3.8)$$

where, t_i^* & t_i^+ are the prior & posterior estimates. Thus the multiple model adaptive filtering algorithm is composed of a bank of j separate Kalman filters, each based on a particular value $a_1 \ldots, a_j$ of the parameter vector, a. When the measurement 'y_i' becomes available at time, t_i, the residuals $r_1(t_i), \ldots, r_j(t_i)$ are generated in the j filters and used to compute the probabilities $p_1(t_i), \ldots, p_j(t_i)$ and also the firing weights $f_1(t_i), \ldots, f_j(t_i)$.

The Kalman filter residuals are given by:

$$r_j(t_i) = y(t_i) - c_j \hat{x}(t_i^*) \quad (3.9)$$

where, t_i * is the prior estimate.

One expects from Equation 3.9, the residuals of the Kalman filter based upon the best model to have mean squared value most in consonance with its own computed covariance, $A_j(t_i)$, while mismatched filters will have larger residuals than anticipated through $A_j(t_i)$. Therefore, the performance of the algorithm depends on there being significant differences in the characteristics of residuals in correct versus mismatched filters. Each filter should be tuned for best performance when the true values of the uncertain parameters are identical to its assumed value for these parameters. One should considerably avoid the conservative philosophy of adding considerable dynamics pseudonoise, often used to open the bandwidth of a single Kalman filter to guard against divergence, since this tends to mask the differences between the good and bad models.

Filter Tuning

The above Equations 3.3 through 3.8 indicates that the state estimation using a Kalman filter consists of two parts, the propagation (Equations 3.7 and 3.8) and measurement update (Equations 3.3 through 3.6) known as 'correction'. Equation 3.7 in the propagation part of the Kalman filter evaluates the contribution of the measured input, propagating through the plant dynamics, to the state estimates. The correction (measurement update) part modifies (updates) the above estimation by the effects of the process and measurement noises.

Every model has a certain amount of uncertainity/nonlinearity. Practitioners normally account for modelling uncertainities by putting extra emphasis on the correction

Every model has a certain amount of uncertainity/nonlinearity. Practitioners normally account for modelling uncertainities by putting extra emphasis on the correction part of the filter through the introduction of some dynamic pseudonoise into the plant. This is in addition to the actual process noise, the plant is exposed to. The summation of the covariances of the actual process noise and the synthesized dynamic pseudonoise will be the process noise covariance (w) used by the filter. It can be seen from equation 3.8 that high values of w result in high error covariance (P) which results in high Kalman filter gain (L); see Equation 3.4. The drawback of this fix is excessive estimation bandwidth which deteriorates the low-pass filtering characteristics of the estimator. Moreover, when the estimator is used in feedback controls, the closed loop system will have very poor stability robustness.

Hence each filter should be tuned for best performance when the true values of the uncertain parameters are identical to their assumed values, as explained above, for reducing the stability robustness of the filter and the controlled system.

Process Noise Characterization

For many physical systems, including active suspension, it may not be justified to assume all the noises (especially) process noises) are white Gaussian (assumed by the Kalman filter). For these systems, it is useful to generate the power spectral density of the real noise data and then develop an appropriate noise model called shaping filters. These filters, which will be augmented to the plant, are driven by white noise processes which they shape to represent the spectrum of the actual noise.

The road input to the active suspension travelling on two types of courses, Letourneau and DAT-P, are considered as process noise in this work. The former

resembles dirt road and the latter resembles a bumpy road. Figure 3.1 shows the uneveness velocity, experienced by the tire travelling at 25 mph, for these courses. The validity of zero-mean assumption of the process noise is clearly indicated in the figure. The whiteness assumption is discussed as follows.

Figure 3.2 shows the power spectrum of road unevenness velocity (process noise) for various Letourneau courses with various unevenness rms's, for the right tire, traversed at 25 mph.

Pure integrators and low-pass filters have been proposed in the literature for shaping the road disturbance in suspension systems. Considering the reasonable flatness of the power spectrum of the disturbance, Letourneau courses unevenness velocities, over the frequency range of interest in suspension problem (<10 HZ), the road process noise is considered 'white' for these courses, with covariance dependent on the vehicle speed and root mean square (rms) of profiles; see Figure 3.3. Knowing the vehicle speed and the road profile, $w_j(t_i)$ in the propagation equation is updated through Figure 5.3. Knowing the vehicle speed and the road profile, $w_j(t_i)$ in the propagation equation is updated through Figure 5.3 (stored in a look-up table). The covariance of the road process noise can also be evaluated, in real-time, via a smearing memory routine fed by the output of a preview sensor.

Figure 3.4 shows the power spectrum of the process noise input to the suspension traversing the DAT-P course at various speeds. The corresponding frequency response of the shaping filters, approximated by double integrators, are also shown on the power spectrum plots of Figure 3.4.

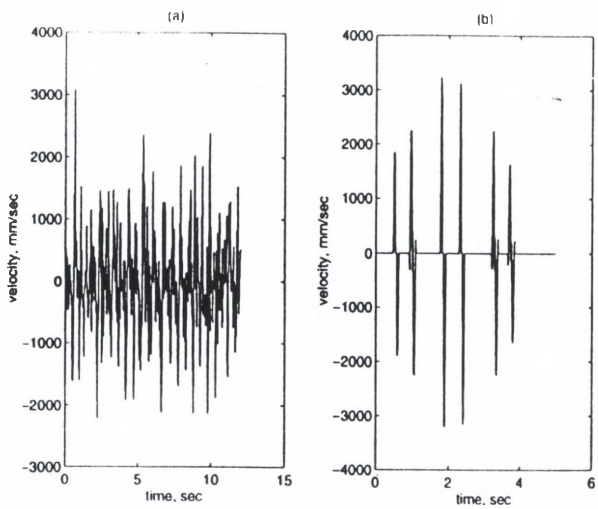

Figure 3.1 - Process Noise; (a) Letourneau Courses and (b) DAT-P Course traversed at 25 mph

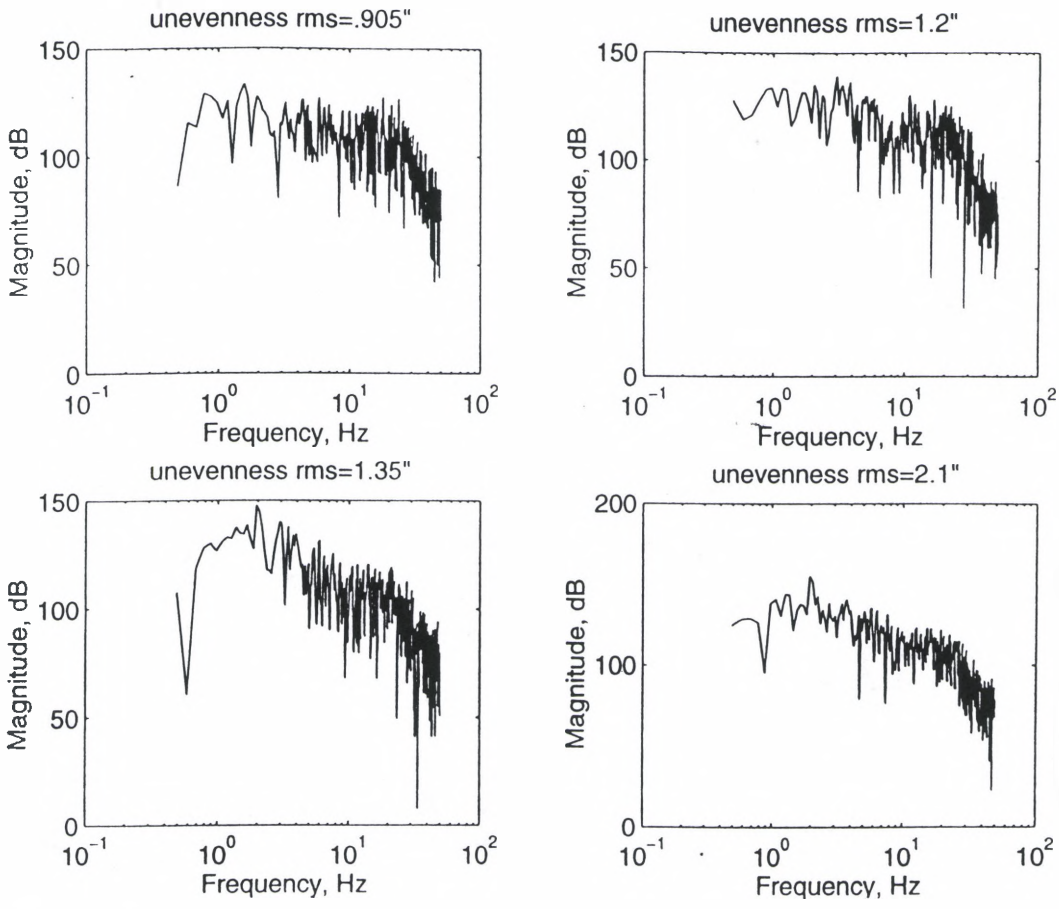

Figure 3.2 - Power Spectrum of Letourneau Courses, for right tire, traversed at 25 mph

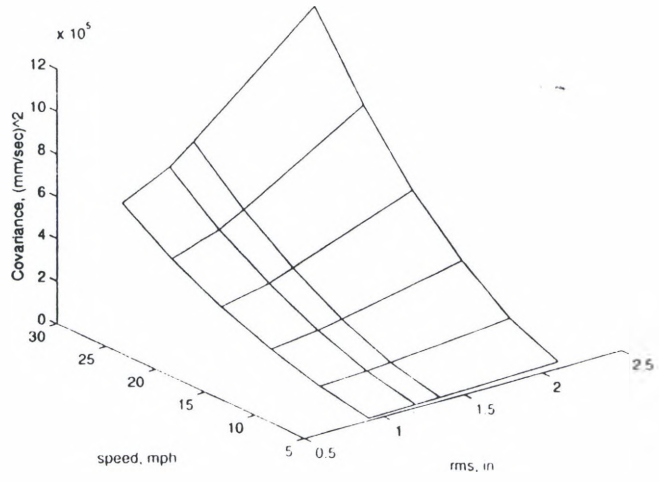

Figure 3.3 - Covariance of the Letourneau Courses process noise

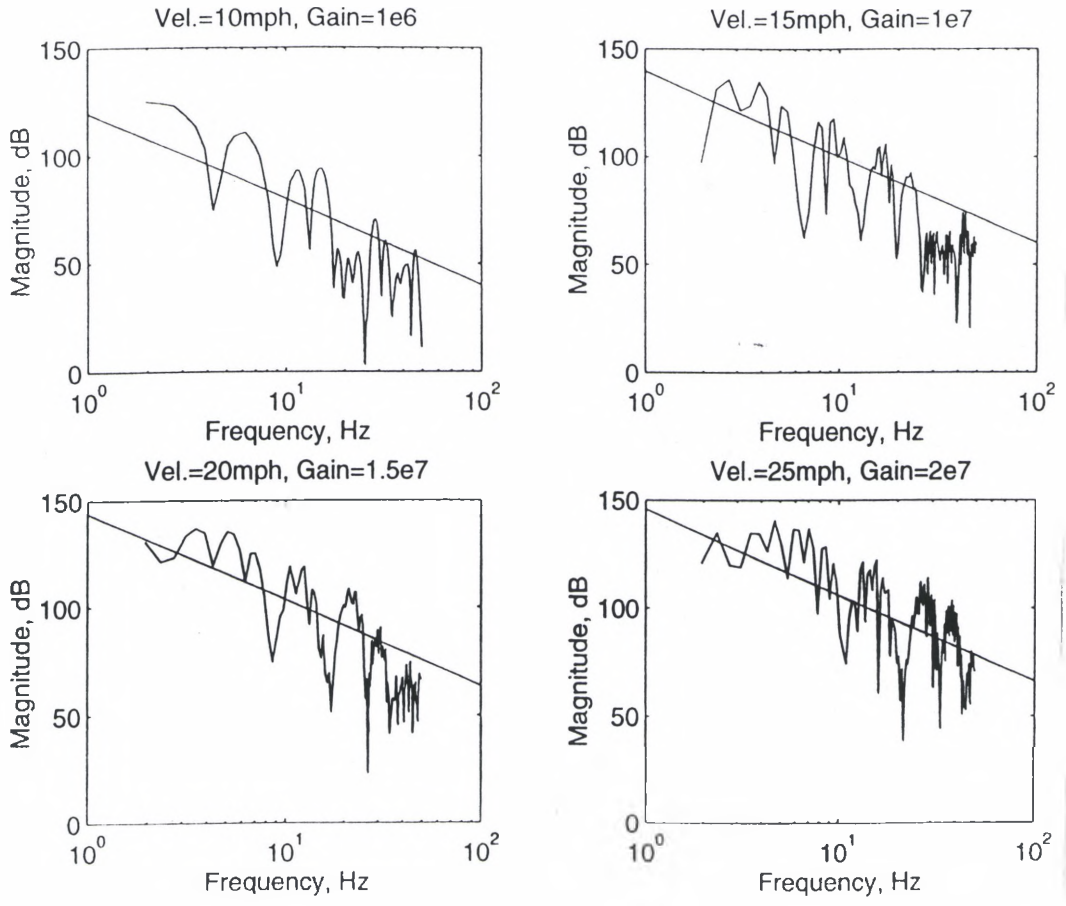

Figure 3.4 - Power Spectrum and Shaping Filters frequency responses of DAT-P Course traversed at various speeds

CHAPTER IV

BLENDING TECHNIQUES

Probability Theory

Multiple model adaptive estimation and control techniques have a structure of a bank of parallel Kalman filters or parallel LQG (linear system model, quadratic cost and Gaussian noise models used for synthesis) controllers that are used to form a state estimate or control output as a probability weighted sum. Each filter or controller is based upon an assumed value of the uncertain parameter **a** to which adaptation is to occur and it is the characteristics of the residuals from each of these filters that allows the evaluation of the probability, based upon the best assumed parameter at the current time. The parameter can affect the matrices defining the structure of the model or depicting the statistics of the noises entering it. In order to make simultaneous estimation of states and parameters tractable, the continuous range of **a** values is discretized into j representative values. If we define the hypothesis conditional probability, pj (ti) as the probability that **a** assumes the value 'a_j' (for j = 1,2,...,J), conditioned on the observed measurement history to time t_i:

$$p_j(t_i) = P_r \{a = a_j \mid y(t_i) = y_i\} \tag{4.1}$$

then it can be shown [1-4] that $p_j(t_i)$ can be evaluated recursively for all j via the iteration:

$$p_j(t_i) = \sum_{j=1}^{J} \frac{f_y(t_i)|a, Y(t_{i-1})(Z_i|a_j, Z_{i-1} \cdot p_j(t_{i-1})}{f_y(t_i)|a, Y(t_{i-1})(Z_i|a_{kj}, Z_{i-1} \cdot p_j(t_{i-1})} \tag{4.2}$$

in terms of the previous values of $p_1(t_{i-1}),....,p_j(t_{i-1})$ and conditional densities for the current measurement $y(t_i)$ to be defined explicitly in 4.12. Notationally, the measurement history random vector $y(t_i)$ is made up of partitions $y(t_1),....,y(t_i)$ that are the measurement vectors available at the sample times $t_1,...,t_i$; similarly, the realization y_i of the measurement history vector has partitions $y_1,...,y_i$. Furthermore, the Bayesian minimum mean square error estimate of the state is the probability-weighted average:

$$\hat{x}_{jj}(t_i^+) = E\{x(t_i) \mid y(t_i) = y_i\}$$

$$= \sum_{j=1}^{J} \hat{x}_j(t_i^+).p_j(t_i) \qquad (4.3)$$

where $\hat{x}_{jj}(t_i^+)$ is the state estimate generated by a Kalman filter based on the assumption that the parameter vector equals a_j. More explicitly, let the model corresponding to a_j be described by an 'equivalent discrete time model' for a continuous time system with sampled data measurements:

$$x_j(t_{i+1}) = \varphi_j\{t_{i+1}, t_i\}\, x_j(t_i) + G_{2j}(t_i)\, u(t_i) + G_{1j}(t_i)\, w_j(t_i) \qquad (4.4)$$

$$y(t_i) = C_j(t_i)\, x_j(t_i) + v_j(t_i) \qquad (4.5)$$

where x_j is the state, u is a control input, w_j is discrete time zero mean white Gaussian dynamics noise of covariance $Q_j(t_i)$ at each t_i, y is the measurement vector and v_j is the discrete time zero mean white Gaussian measurement noise of covariance $R_j(t_i)$ at t_i, assumed independent of w_j; x_{t0} modelled as Gaussian, with mean x_{j0} and covariance P_{j0} and is assumed independent of w_j and v_j.

Using the measurement update and the propagation relation as explained in

Chapter 3, the Kalman filters are designed. Each numerator density function in Equation 4.2 is given by:

$$f_y(t_i)|a, Y(t_{i-1})(Z_i|a(j), Z_{i-1} = \text{Exp}\{5 * r_j'(t_i).F_j^{-1}(t_i).r_j(t_i) / 2\prod^{1/2m*|F_j(t_i)|^{1/2}}\}$$

(4.6)

where **m** is the measurement dimension and $A_k(t_i)$ is calculated in the j^{th} Kalman filter as mentioned in the measurement update equations. The denominator in 4.2 is simply the sum of all the computed numerator terms and thus is the scale factor required to ensure that the $p_j(t_i)$ is sum to one. If this is not taken care, then the probability weighting would sum up to greater than one and this would cause stability problems since more control input is given than necessary.

The other blending technique is **Fuzzy Logic**, which is explained in detail in Appendix A.

Residual Monitoring

Each Kalman filter residual rj, is defined as

$$r_j(t_i) = y(t_i) - C_j \hat{x}(t_i^-) \quad (4.7)$$

The residual is ideally (when there is no model uncertainity) a white, Gaussian, zero mean, sequence of covariance F_j in the measurement update equation. Moreover, P_j of the same equation describes the optimal covariance matrix of the state estimation error $x(t_i) - \hat{x}(t_i^-)$ in the measurement update equation. Likelihood quotient shown in Equation

34, q, compares of the residual, r_j, with the filter's internally computed residual covariance, F_j.

$$q_j = r_j^{'}(t_i)\, F_j(t_i)^{-1}\, r_j(t_i) \qquad (4.8)$$

q is merely the sum of scalar terms relating the product of any two components of the residual vector and the internally computed covariance for those two components. Considering that the 'mismatched' filters (filters based on less perfect models) will have larger residuals than anticipated through F_j, filters with residuals that have square values most in consonance with their internally computed covariance are the most 'matched' filters. These filters are weighted more heavily in calculations of the control.

The above mentioned scalar terms or their sum (likelihood quotient, Equation 4.10) are used as the auxilliary input(s) to the fuzzy logic scheme that evaluates the control input to the suspension by blending the individual Kalman filter-based (LQG) controls. They are both viable indications of how good the estimation of each filter, at any point in time, is.

Also, the switching mechanism is based on a threshhold value of the residuals from each of the filters. This mechanism serves as an important scheme in model stability. It could go unstable when the state estimate from one of the filters starts sinking even when the car is on the ground and when the state estimate from the other two filters starts building up when the car is off the ground. This is explained in detail in Chapter VI.

Stability Analysis by Monte Carlo Method

The parameters of the suspension namely ϕ = [M, m, K, Kt, C, Ct] vary

depending on various factors, e.g. the viscosity of oil changes due to the temperature variation, resulting in the damping coefficient variation. Also the tire stiffness and the damping coefficient changes with respect to the tire pressure, vehicle speed etc., These parameters contribute to the model uncertainity of the quarter car system and they have a significant influence on its fidelity.

The variation of these variables are not known specifically and can be estimated by Monte Carlo Analysis. The nominal values or the mean of each parameter is initially specified. We assume that the parameters have a normal distribution with the mean, μ and variance, v. The variance of the vector, ϕ for the Monte Carlo simulation is taken as 5% of the mean. Knowing the variance and the mean, the unknown parameter values are found as estimates, $(X) = z*v + \mu$ for each suspension parameter, where **z** is a normally distributed random variable.

Random values representing the probability, p are chosen for each suspension parameter. The values of probability, p, between (0 & 0.5) would represent a normally distributed random variable, z, between (5 & 0). The probability, p, between (0.5 & 1) would represent a normally distributed random variable, z, between (0 & -5) thus having the span of the probability, p, is between (0 & 1) corresponding to the span of the normally distributed random variable, z, between (5 & -5).

The look up table mapping p to z are fed into the computer with a written code. This process is necessary to automatically fire a random variable value for each suspension parameter, whose probability is known at a given time. The probability values are normally assumed for each suspension parameter statistically.

Each controller is designed based on a fixed value of ϕ. The randomly selected parameters found by Monte Carlo Analysis is coupled along with the plant model, and used in the simulation of the controlled system. Eight runs are used to indicate the stability of the system. Figure 4.1 depicts tbe rattlespace of the active suspension corresponding to the 8 runs discussed above.

CHAPTER V

SIMULATION RESULTS

The non linear dynamics of the quarter car suspension is modelled using Equations of state variable formulation. The model is used to analyze the LQG-based fuzzy logic controller developed in this work. The stiffness and damping coefficient of the tire are the only nonlinearities of the current model. The suspension model is approximated by 3 linear models considering constant tire stiffness and damping coefficients evaluated at the three tire deflections of 0.04, 0.025 and 0.01 m (practically zero), measured relative to the unloaded tire position. These linear models are used for augmenting the suspension with a low-order approximation of human body response filter. The bank of optimal controllers are designed using these augmented linear models. The same linear models are also used in the bank of estimators, providing the state estimates of the suspension to the controller. The states of the human body response filter is measured by running the measured acceleration of the sprung mass through the 2nd order filter. These states are provided to the bank of controllers. Note that the added filter states do not add extra computational burden on the bank of estimators. The measurements used in driving the Kalman filters are the working space of the suspension and the actuator force. Sprung mass acceleration will be added to the measurement vector and will be fed to the estimators in the future. The residual of each estimator is squared and scaled by its internally computed covariance

in each estimator and used as the input to the fuzzy logic blending algorithm which mixes the control provided by each controller. This control will drive the nonlinear suspension model described above.

Open and closed-loop integrated squared acceleration (the square of the sprung mass acceleration is integrated over time, i.e., $\int_0^{\infty} (acc^2\, dt)$, which indicates the absorbed power and working space, in response to 1.35" RMS Letourneau course traversed at 25 mph, for the following two sets of weights are shown in Figures 5.1 and 5.3. The corresponding control actuations are depicted in Figures 5.2 and 5.4. Note that the weight set 1 has more emphasis on minimizing the working space (higher rho 2).

$[\text{rho } 1....\text{rho } 4]_1$ = [1e0 1e2 1e-8 1e0]

$[\text{rho } 1....\text{rho } 4]_2$ = [1e1 1e-1 1e-8 1e0]

Comparison of the squared sprung mass acceleration on open (passive) and closed loop suspension indicates that using a high weight on working space, i.e., weight set 1, the absorbed power is reduced to half while the suspension travel is also reduced; see Figure 5.1. By reducing the weight on suspension travel in the objective function, e.g., weight set 2, the absorbed power is dramatically reduced without any increase in suspension travel beyond that of the open loop system; see Figure 5.3.

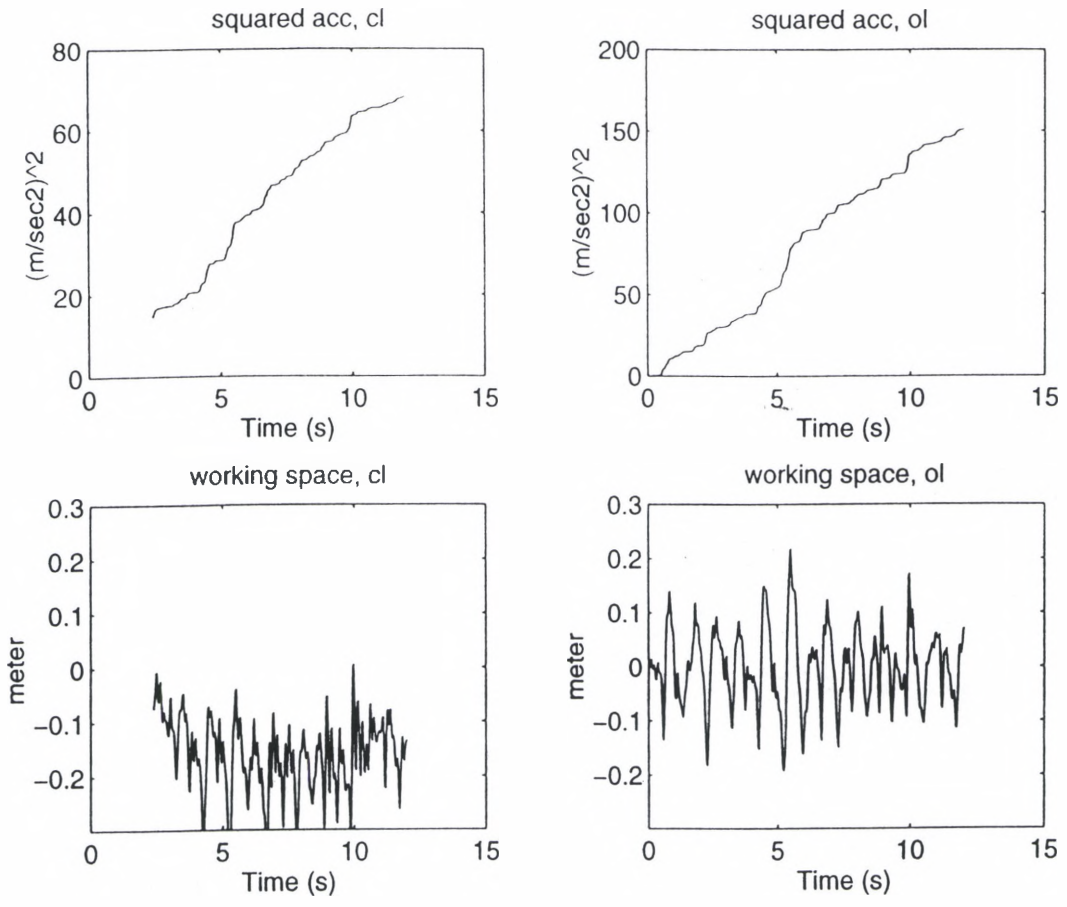

Figure 5.1 - Open and Closed loop integrated squared sprung mass acceleration and working space using weight set 1

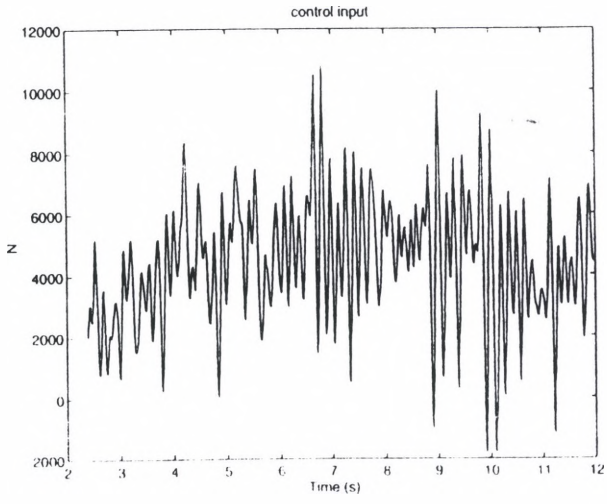

Figure 5.2 - Closed loop control actuation using weight set 1

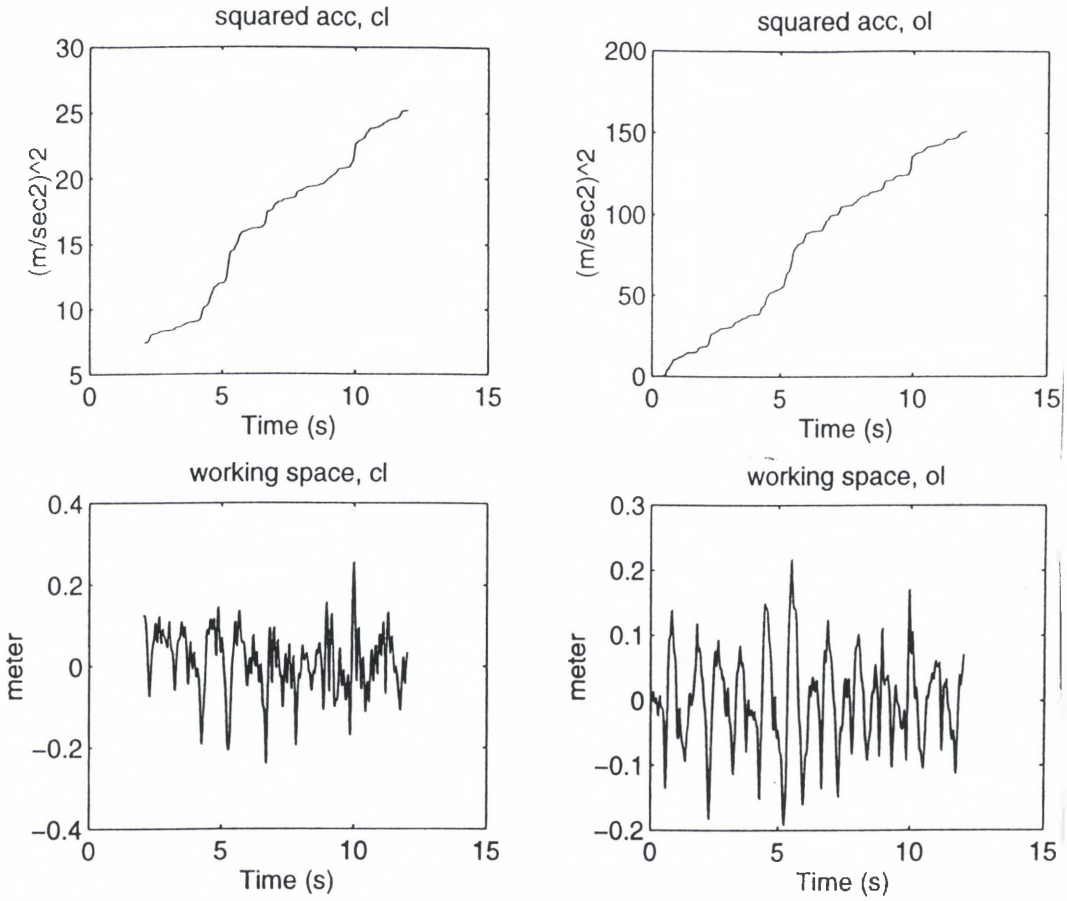

Figure 5.3 - Open and Closed loop integrated squared sprung mass acceleration and working space using weight set 2

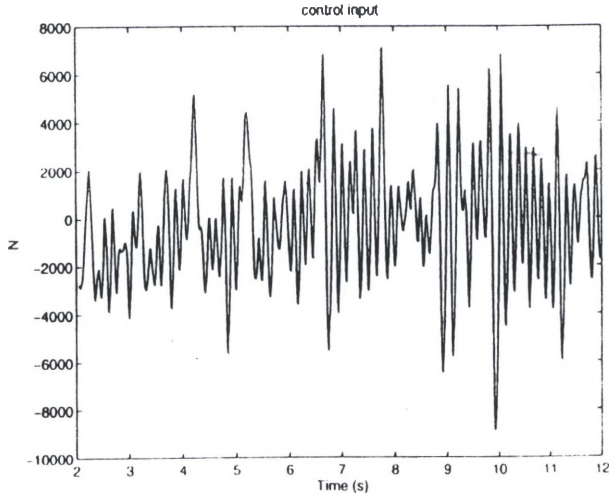

Figure 5.4 - Closed loop control actuation using weight set 2

CHAPTER VI

SUMMARY, CONCLUSIONS AND RECOMMENDATIONS FOR FURTHER RESEARCH

Summary and Conclusions

Design of active car suspension system thrusts its objective in reducing the absorbed power while simultaneously improving the road contact with a minimal suspension rattlespace. The problem of improving comfort and road contact is the dominating question in literature on active suspension system design for more than twenty years. Although the nature of the system makes this particular problem so outstanding among the other suspension objectives, that a passive suspension is incapable of providing a sufficient solution, e.g. for the demand of a horizontal position of the car during curving. This demand requires an infinite stiffness of the suspension spring and of the tire, which is unrealistic and not desirable, whereas it is a simple regulator problem or a question of zero steady state error, if an active element is employed. In the case of trade off between comfort and road contact, however, a decent solution is provided by a passive suspension, so that the demand on an active element is that of improving the given solution. In Chapters 1 and 2, a cross-section of the publications of the last 23 years is given, which leads to the conclusion, that neither LQR methods nor conventional

matching of the skyhook suspension yield sufficient results under the constraints of limited measurements and necessity of a not fully active suspension.

In Chapters 3 through 4 an alternative, LQG based fuzzy logic control of active suspension system, is discussed and its formulation for active car suspension is developed. This finally results in a controller design which has good performance and sufficient stability robustness. The only necessary measurement is that of measuring the distance between the sprung and the unsprung masses, which is very easy to obtain and accurate.

Recommendations for further Research

The main objective of this work was to find a control method which improves comfort and road contact simultaneously based on practical assumptions for the model, namely limited measurements and avoidance of the necessity of a fully active suspension. For the quarter car model, the control technique namely LQG-Based Probabilistic Control of Active Suspension is implemented and compared to Fuzzy Logic. These techniques are not the best, hence further research on control strategy is strongly recommended.

Though our control strategy provided good results for the objectives of comfort and road contact on a quarter car model, its abilities on a full car model with additional objectives like roll and pitch behaviour, needs to be explored. A simple model, incorporating a full car is, shown in Figure 6.1. Note that this model has four independent road disturbance inputs whereas in reality the inputs of the front and rear are correlated: the rear input is a time delayed version of the front disturbance input. Therefore the system has only two independent road disturbance inputs, one on the right

and the other on the left side. Analysis of possibilities to improve the system by utilizing the knowledge from the front for the rear suspension is another topic for further research.

An important part for further research is how model order reduction of the controller affects the properties of the active suspension system. The order of the controller increases drastically due to more states of the full car system, actuator dynamics, more and complicated weighting functions.

In our work, all the simulations of the system have been done on Matlab and Simulink. Further testing, especially for full car models, should be done with a full car simulator, which incorporates a good approximation for the tire, e.g. modelling of the surface contact and other neglected features such as saturation due to limited working space, limited contraction of the tire or limited force provided by a real actuator.

One important application area for multiple model algorithms is the adaptive control of the automobile system namely the High Mobility Multipurpose Wheeled Vehicle (HMMWV). For this case, the use of a 'moving-bank' multiple model estimation and/or control algorithm has been investigated. Rather than implementing parallel filters or controllers based upon all viable discrete parameter values for all time, only a subset of these discrete values is used at any one time. Also, implementing the multiple model in parallel has an adverse effect, since one of the filters based on 'off-road' condition tends to sink even when the model is on the ground, which leads to unstability. This prompted us to have a dynamic logic that decides which subset of values should be currently implemented.

This concept was further made easier since we had to consider a maximum of 3 separate filters. Maintaining fewer elemental filters in the bank enhances the feasibility

of the algorithm but could aggravate the behaviour observed earlier in fixed-bank algorithms of making inappropriate decisions when the true model is not included in the model set of the filter. Some research has been directed at the information theoretic problem associated with this condition and further recent research has portrayed the performance capabilities of various proposed decision logics for 'moving' (and changing the size, if more number of filters are used, but not in this work) the bank of currently used values around the parameter space [26].

This research [26] has addressed the robustness issues of such an adaptive estimator/controller. A final implementable controller will necessarily be based upon reduced-order, simplified models in order to maintain reasonable computational loading.

As discussed above, since our work has 3 filters and only one parameter varying namely the tire deflection, only 3 filters and controllers have to be implemented. Each filter design is based on a vector of uncertain parameter 'a', which is dependent on the tire deflection (road contact) alone. Three values of tire deflection are arrived at by dividing equally the range of tire deflection and approximating by its midpoint. This produces 3 separate filters tuned to their regions alone producing the best result. One of the regions is considered to be off the ground by choosing the tire deflection (K_t) and the damping coefficient(C_t) to be zero, whereas the other two regions are considered to be on the ground with suitable values for K_t and C_t.

The problem with this type of approach is that all the 3 filters run simultaneously disregard to whether the car is on or off the ground. Either way the estimation is wrong, since if the car is on the ground, one of the filters predicts it still to be off the ground and gives the wrong estimation of the states. If the car is off the ground then two of the filters

predict it to be on the ground again giving a wrong estimation. To solve this problem, a suitable switching logic is proposed based on the residual. Consider the same problem as discussed above. If the car is on the ground, then one of the filters predicts it to be off the ground, which would give a higher residual value since the estimated output would be away from the measured output unlike the other two filters which would have a smaller residual since the estimated output falls in line with the measured output. If the car is now off the ground, then two of the filters predicts a higher residual whereas the third filter predicts a lower value. The filters corresponding to the car on the ground is one set, whereas the third filter corresponding to the car off the ground is taken as the second set.

Switching is done in such a way that a previous history of the measurement of residuals are plotted and their values noted for each of the filters. If the residual value exceeds a threshhold value, decided by a history of measurements, then switching is done from one set to another. It implies that the Kalman filter itself stops estimating, since that would cut down computational time on the computer. Care is also taken that, even if the filter starts running for whatever reason, when it is not supposed to, the final output of the states is still zero, brought about by a suitable decision logic function. This mechanism would certainly improve the stability of the model, since shutting off one of the set of filter or filters would stop the model from sinking or building up (adding up).

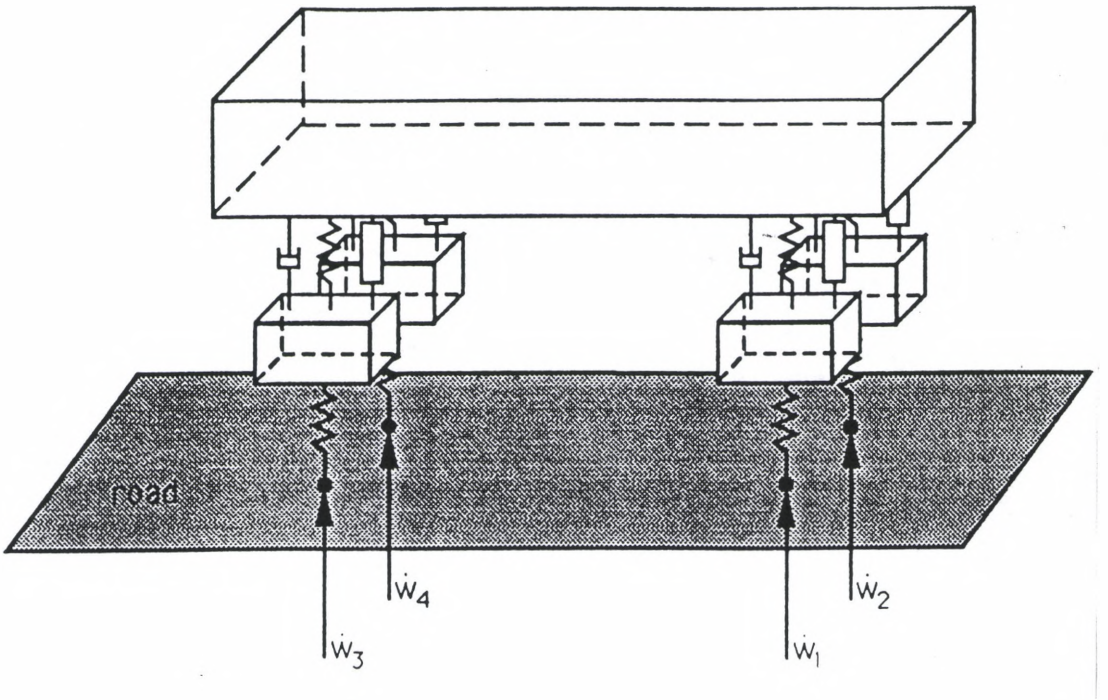

Figure 6.1 - Full Car Model with four independent road inputs

REFERENCES

[1] Al-Assaf, Yousef, "Adaptive Control for vehicle active suspension systems", Proceedings of the 1995 American Control Conference, v 2, 1995.

[2] Anderson, B.D.O. and Moore, J.B., "Optimal Control", Prentice Hall Information and System Science Series, Prentice Hall, 1990.

[3] Captain, K.M., Boghani, A.B. and Wormley, D.M., "Analytical Tire Models for Dynamic Vehicle Simulation", Vehicle System Dynamics, Vol. 8, 1979, pp. 1-32.

[4] Clark, S.K., "Mechanics of Pneumatic Tires", rev. ed., U.S. Department of Transportation, National Highway Traffic Safety Administration.

[5] Dailey, R.L., "Lecture notes for the workshop on H-Inf and Mu Methods for Robust Control", American Control Conference, May 21- 22, 1990, San Diego, California.

[6] Doyle, J.C., "Analysis of Feedback Systems with Structured Uncertainities", Proc. IEEE-D, 1982, pp. 242-250.

[7] Doyle, J.C.and Stein, G., "Multivariable Feedback Design: Concepts for a Classical/Modern Synthesis", IEEE Trans. On Automatic Control, AC-26, February, 1981, pp. 4-16.

[8] Eiler, M.K.and Hoogterp, F.B., "Analysis of Active Suspension Controllers", Summer Computer Simulation Conference, July 1994, San Diego, California.

[9] Grigg, F.W., "The Radical Stiffness and Damping Properties of Pneumatic Tires", Mechanical and Chemical Transactions, Institute of Engineers, Australia, 1967, pp. 239-244.

[10] Hac, A., "Suspension Optimization of a 2-DOF Vehicle Model using a Stochastic Optimal Control Technique", Journal of Sound and Vibration, Vol. 100, No. 3, 1985, pp. 343-357.

[11] Hac, A., "Adaptive Control of Vehicle Suspension", Vehicle Suspension Dynamics, 16, 1987, pp. 57-74.

[12] Hashiyama, T., Behrendt, S., Furuhashi, T. And Uchikawa, Y., "Fuzzy Controllers for semi-active suspension system generated through genetic algorithms",

Proceedings of the 1995 IEEE International Conference on Systems, Man and Cybernetics, 1995, pp. 4361-4366.

[13] Hrovat, D. and Hubbard, M., "Optimum Vehicle Suspensions minimizing RMS Rattlespace sprung mass acceleration and Jerk" Trans. A.S.M.E. Journal of Dynamic Systems, Measurement and Control, Vol. 103, September, 1981, pp. 228-236.

[14] Ivers, D.E. and Miller, L.R., "Experimental Comparison of Passive, semi-Active On/Off and Semi Active Continuous Suspensions", Truck and Bus Meeting and Exposition, Charlotte, North Carolina.

[15] Karnopp, D., "Active Damping in Road Vehicle Suspension Systems", Vehicle System Dynamics, Vol. 12, 1983, pp. 291-311.

[16] Karnopp, D., "Theoritical Limitations in Active Suspensions", Vehicle System Dynamics, Vol. 15, 1986, pp. 41-54.

[17] Kiriczi, S.B. and Kashani, R., "Control of Active Suspension with Parameter Uncertainity and Non-White Road Uneveness Disturbance Input", SAE Publication No. 902283.

[18] Kiriczi, S.B. and Kashani, R., "Robust Control of Active Car Suspension with Model Uncertainity using H-Inf Methods", Advanced Automotive Technologies, Velinsky et. Al. Eds., DE-Vol. 40, The ASME BK. # H 00 719, 1991, pp. 375-390.

[19] Kiriczi, S.B., "Robust Control of Active Car Suspension using H-∞ Methods", M.S. Thesis, Michigan Technological University, 1991.

[20] Laub, A.J., "A Schur Method for solving Algebraic Riccati Equations", IEEE Transactions on Automatic Control, Vol. AC-24, 1979, pp. 913 - 921.

[21] Laub, A.J. and Little, J.N., "Control System Toolbox", Matlab Control System Toolbox, 1986.

[22] Lee, A.Y. and Salman, M.A., "On the Design of Active Suspension Incorporating Human Sensitivity to Vibration" Optimal Control Applications and methods, Vol. 10, 1989, pp. 189-195.

[23] Maciejowski, J.M., "Multivariable Feedback Design", Addison-Wesley Publishing Company, 1989.

[24] Magill, D.T., "Optimal Adaptive Estimation of Sampled Stochastic Processes", IEEE Trans. on Automatic Control, Vol. 10, 1985, pp. 434-439.

[25] Margolis, D.L., "Semi-Active Control of Wheel Hop in Ground Vehicles", Vehicle System Dynamics, Vol. 12, 1983, pp. 317-330.

[26] Maybeck, P.S. and Schore, M.R., "Reduced-Order Multiple Model Adaptive Controller for Flexible Spacestructure", IEEE Trans. on Aerospace and Electronic Systems, Vol. 28, July, 1992.

[27] Rotea, M.A. and Khargonekar, P.P., " Simultaneous H2/H-Inf Optimal Control with State Feedback", American Control Conference, San Diego, California, 1990, pp. 2380-2384.

[28] Sharp, R.S. and Crolla, D.A., "Road Vehicle Suspension Design - A Review", Vehicle System Dynamics, Vol. 16, 1987, pp. 167-192.

[29] Sharp, R.S. and Hassan, S.A., "The Fundamentals of Passive Automotive Suspension System Design" Society of Environmental Engineers Conference on Dynamics in Automotive Engineering, 1984, pp. 104-115.

[30] Stein, G. and Athans, M., "The LQG/LTR procedure for Multivariable Feedback Control Design", IEEE Trans. On Automatic Control, AC-32, February, 1987.

[31] Tamai, Edilson H. and Sotelo, Jose Jr., "LQG - Control of Active Suspension considering vehicle body flexibility", Proceedings of the 1995 IEEE Conference on Control Applications, v 2, 1995, pp. 143 - 147.

[32] Thompson, A.G., "Optimal and Suboptimal Linear Active Suspensions for Road Vehicles", Vehicle System Dynamics, Vol. 13, 1984, pp. 61-72.

[33] Thompson, A.G. and Davis, B.R., "Optimal Active Suspension Design using a Frequency Shaping PID Filter", Vehicle System Dynamics, 21, 1992, pp. 19-37.

[34] Ulsoy, A.G. and Hrovat, D., "Stability Robustness of LQG Active Suspensions", American Control Conference, San Diego, California, May 23-25, 1990, pp. 1347-1356.

[35] Wilson, D.A., Sharp, R.S. and Hassan, S.A., "The Application of Linear Optimal Control Theory to the Design of Active Automotive Suspension", Vehicle System Dynamics 15, 1986, pp. 105-118.

[36] Yamaguchi, J., "Nissan and Toyota adopt Active Suspension on Production Cars", Automotive Engineering, December, 1989, pp. 86-90.

APPENDIX A

Fuzzy Logic Controller

At any given point in time, the non linear suspension model can be approximated by a set of linear models, with varying degrees on each element of the set. Let the vector of uncertain parameters in the linear stochastic state model of Equation 1.9 be denoted by, a = [Ct Kt]'. Both these parameters are functions of tire deflection, x2 only. The range of x2 can be discretized into J representative values for implementation reasons resulting in J sets of uncertain parameter vector pj (for j = 1,2, ..., J). In this work, x2 is divided into J = 3 regions and the center of each region is chosen to evaluate each aj. This discretization results in 3 linear models thereby giving 3 Kalman filters and 3 LQ feedback gain vectors, along with the necessary fuzzification, rule base and the defuzzification elements, as shown in Figure 2.1. Each LQG controller, designed for each linear model, is then fired with its corresponding firing weight. The fuzzy input variable to the rule set is the residuals of each Kalman filter properly scaled by their internally computed covariances.

Fuzzy Logic

The fuzzy logic is used to blend the individual control actions generated by the bank of LQG controllers shown in Figure 2.1(a). The mechanics of this blending is described below:

The Input Space

The input to the fuzzy logic controller is the comparison of the residual covariance for each filter with the filter's internally computed residual covariance. This input is the likelihood quotient, q described by Equation 1.

$$qj = rj'(ti)\, Fj(ti)\, inv\, rj(ti) \qquad (1)$$

q is merely the sum of scalar terms relating the product of any two components of the residual vector and the internally computed covariance for those two components. Considering that the 'mismatched' filters (filters based on less-perfect models) will have larger residuals than anticipated through Fj, filters with residuals that have square values most in consonance with their internally computed covariance are the most 'matched' filters. These filters are weighted more heavily in calculations of the control. The above-mentioned scalar terms or their sum (likelihood quotient, Equation 1) are used as the auxillary input(s) to the fuzzy logic control scheme that evaluates the control input to the suspension by blending the individual Kalman filter-based (LQG) controls.

The universe of discourse for 'q' is the range of all possible covariances of the residuals, with the minimum value of zero. Assuming the maximum of the range in q is +10, the universe of discourse is:

$$Uq = (0,10) \qquad (2)$$

The universe of the fuzzy variable must be covered with fuzzy sets that represent all possible fuzzy values the variable can assume. Trapezoidal representations are used as the membership functions of the fuzzy inputs sets.

Term Sets of the Inputs

The term set is the set of fuzzy values which a fuzzy variable may assume. In order to keep the potential size of the rule base small, a term set of size 4 was decided upon. Note that as part of tuning the Fuzzy Logic Controller (FLC), the

size of the term set can vary. The four sets defined for the input **q** universe are shown in Figure 1. Each fuzzy set is named as shown in this figure and listed in Table 1(a).

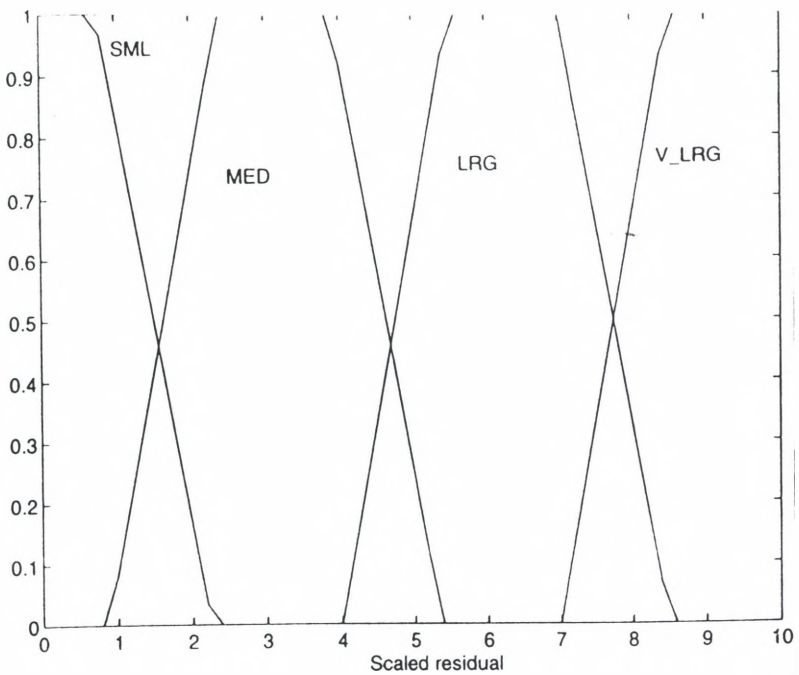

Figure A.1 - Term Sets for the fuzzy input 'q'

Fuzzy set	Description
SML	Small residual
MED	Med residual
LRG	Large residual
V_LRG	Very large residual

TABLE A.1 (a) - Fuzzy input sets and associated descriptions

Input r_c	Output (firing weight)
SML	HIGH
MED	MED
LRG	LOW
V_LRG	ZERO

(b) Rule Base for firing factor

Fuzzification

The fuzzification operation consists of converting the deterministic input, or **q**, to a fuzzy singleton, and then intersecting it with each of the fuzzy sets on the universe of discourse. Because of the nature of the fuzzy singleton (degree of one at the deterministic input and zero everywhere else), and since the membership curve will always have a value less than or equal to one, values equivalent to the intersection can be obtained by plugging the deterministic input directly into the membership function equation for each fuzzy set and solving for the corresponding degree of membership.

Rule Base

The rule base for the FLC must contain information that decides on the extent of firing of each LQG controller for each possible fuzzy input. Table 1(b) shows the format of the rule base. The fuzzy sets describing the rules 'High', 'Med', 'Low' and 'Zero' are shown in Figure 3. The universe of discourse for these rules is between zero, i.e., Zero, (no firing) and 1, i.e., High, (full firing).

The thinking behind the selection is simple and as follows: The fuzzy set 'High', large firing, should be used when the residual is very small indicating the accurate estimation by the Kalman filter.

Note that the two rules, 'Zero' and 'High' are singletons, i.e., they are nonzero only at a single point on the universe. Figure 4 shows the rule base considered for this problem, graphically. It should be emphasized that all the aspects of setting up the rule base are the subjects of controller tuning.

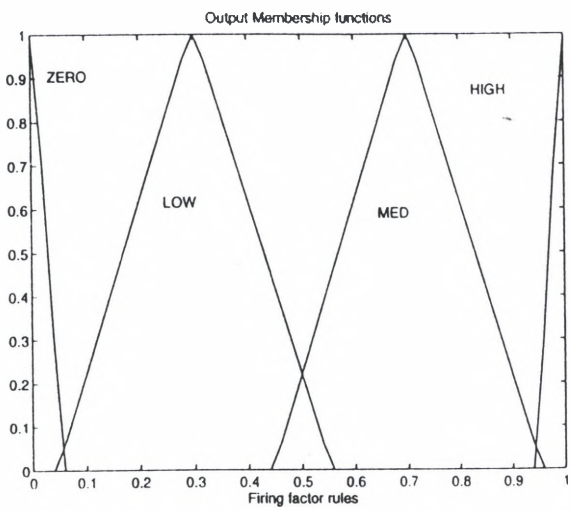

Figure A.2 - Firing factor rules

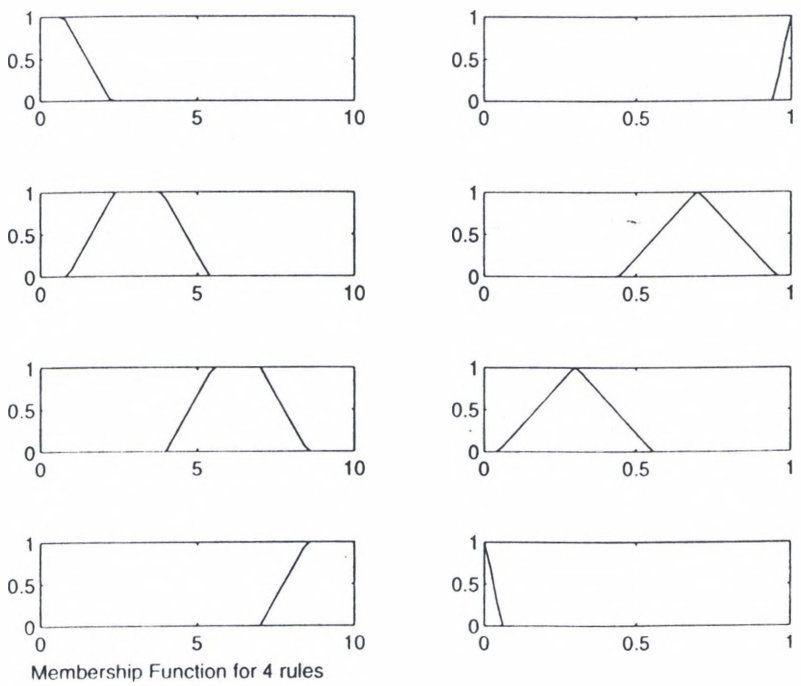

Figure A.3 - Input/Output Rule Base; 1st column (Residual Covariance), 2nd column (Output; firing factor)

Defuzzification

The final aspect of the design consists of using a defuzzification algorithm. Center of area method is used in the simulation presented here. This technique is based on evaluating the center of the area of the union of each inferred output. Using the steps described above, the firing weight curve is evaluated and shown in Figure 4.

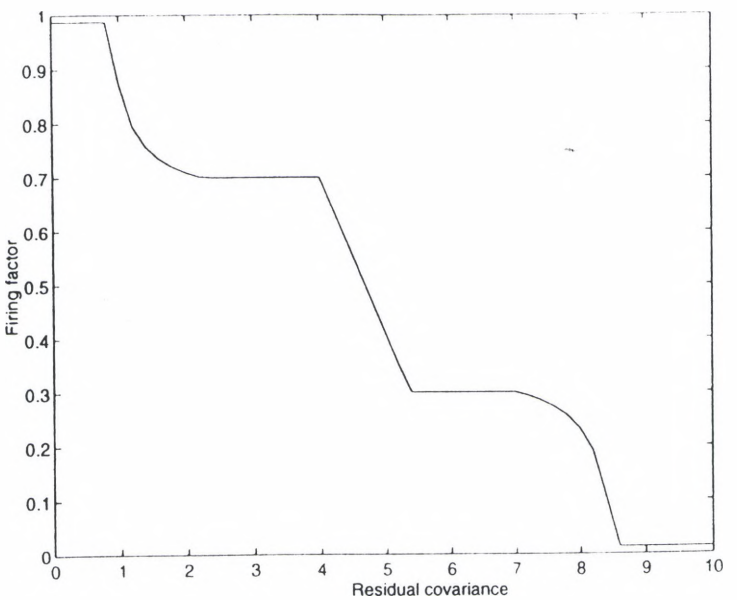

Figure A.4 - Firing weight surface